UNIVERSITAT POLITÈCNICA DE CATALUNYA
BARCELONATECH
Facultat d'Òptica i Optometria de Terrassa

GRAU EN ÒPTICA I OPTOMETRIA

TREBALL FINAL DE GRAU

"TECHNOLOGY FOR DRY EYE DIAGNOSE"

CARLA BARNERA LLORÀ

MIKEL ALDABA AREVALO
JOAN GISPETS PARCERISAS
Departament d'òptica i optometria

Terrassa, 12 de Juny del 2019

UNIVERSITAT POLITÈCNICA DE CATALUNYA
BARCELONATECH
Facultat d'Òptica i Optometria de Terrassa

GRAU EN ÒPTICA I OPTOMETRIA

El Sr. Mikel Aldaba Arévalo, com a tutor del treball y el Sr. Joan Gispets Parcerisas com a director del treball.

CERTIFIQUEN

Que la Sra. Carla Barnera Llorà ha realitzat sota la seva supervisió el treball "Technology for dry eye diagnose" que es recull en aquesta memòria per optar al títol de grau en Òptica i Optometria.

I per a que consti, signo/em aquest certificat.

Sr Mikel Aldaba Arevalo
Tutor/a del treball

Sr Joan Gispets Parcerisas
Director/a del treball

Terrassa, 12 de Juny de 2019

GRAU EN ÒPTICA I OPTOMETRIA

ACKNOWLEDGEMENT

I would like to express my thanks and gratitude to all the people that have helped me in completing my final bachelor's degree final thesis.

First of all, I am very thankful to my project tutor, Dr. Mikel Aldaba Arevalo, for his valuable guidance and his faith in me to effectuate this project, as well as to the director project, Dr. Joan Gispets Parcerisas.

I would like to express my deep sense of gratitude to Ahmed Sherry for his kindness, generosity and support throughout the making of the study. Without him, the project wouldn't have been that pleasant.

I would also like to sincerely thank Ana Rodriguez for her generosity in providing me with the required knowledge on specific fields.

Finally, to my relatives, friends and everyone who in one way or another shared their support and patience with me, thank you.

GRAU EN ÒPTICA I OPTOMETRIA

TECHNOLOGY FOR DRY EYE DIAGNOSE

RESUM

L'afectació de l'ull sec és una de les condicions oculars més freqüents. Tot i la seva importància, els mètodes diagnòstics utilitzats presenten certes limitacions, és per això que avui dia no existeix cap referència clara per a la diagnosis de l'ull sec. Per aquest motiu, són necessàries noves tecnologies econòmiques i no invasives per a l'ús clínic. Així doncs, des del CD6-UPC es va proposar un nou mètode per a diagnosticar el síndrome de l'ull sec, basat en la degradació de la imatge del reflex corneal. Malgrat la nova proposta, el nou sistema presentava una limitació en l'àrea de mesura, ja que era massa petita.

L'objectiu d'aquest projecte era millorar el sistema esmentat anteriorment, augmentant el diàmetre de l'àrea de mesura amb un nou disseny òptic. Aquesta nova configuració va mostrar un comportament semblant al de l'anterior sistema. Tot i així, el diàmetre de l'àrea mesurada era més petit que el calculat teòricament. Es van estudiar diverses raons que podrien explicar aquest inconvenient: la distribució Gaussiana de la intensitat del làser, el mateix làser i la lent d'incidència utilitzada. Els resultats obtinguts suggereixen que la lent d'incidència hi podria influir, per tant, si en futurs projectes es treballa aquest aspecte, es podria arribar a trobar una solució. A més a més, també es va observar que el sistema era molt sensible a petits descentraments del pacient, la qual cosa també podria millorar-se en propers treballs.

GRAU EN ÒPTICA I OPTOMETRIA

TECHONOLOGY FOR DRY EYE DIAGNOSE

RESUMEN

El síndrome del ojo seco es una de las condiciones oculares más frecuentes. A pesar de su importancia, los métodos diagnósticos utilizados presentan ciertas limitaciones, es por eso que hoy en día no existe ninguna referencia clara para la diagnosis del ojo seco. Por este motivo, se necesitan nuevas tecnologías económicas y no invasivas para el uso clínico. De esta forma, en el CD6-UPC se propuso un nuevo método para diagnosticar el síndrome del ojo seco, basado en la degradación de la imagen del reflejo corneal. Pese a la nueva propuesta, el nuevo sistema presentaba una limitación en el área de mesura, era demasiado pequeña.

El objetivo de este trabajo era mejorar el sistema mencionado anteriormente, aumentando el diámetro del área de mesura con un nuevo diseño óptico. Esta nueva configuración mostro un comportamiento parecido al del anterior sistema. Aun así, el diámetro del área mesurada era mas pequeño que el calculado teóricamente. Se estudiaron diversas razones que podrían explicar este inconveniente: la distribución Gaussiana de la intensidad del laser, el propio laser i la lente de incidencia utilizada. Los resultados obtenidos sugieren que la lente de incidencia podría influir, por lo tanto, si en futuros proyectos se trabaja en este aspecto se podría llegar a una solución. Además, también se observó que el sistema era muy sensible a descentramientos del paciente, lo cual también se podría mejor en futuros trabajos.

GRAU EN ÒPTICA I OPTOMETRIA

TECHNOLOGY FOR DRE EYE DIAGNOSE

ABSTRACT

Dry Eye Disease (DED) is one of the most commonly clinically diagnosed ocular conditions. Despite its importance, the diagnostic methods suffer due to significant limitations. Thus, currently, there is still no gold standard method used for dry eye diagnosis and new inexpensive and easy to use tools are required in clinical practice. In this sense, a new method for DED diagnosis based on corneal reflex image degradation was proposed at CD6-UPC. However, this new technique currently presented a limitation, as its measured area was too small.

The aim of this work was to improve the previously mentioned setup designed by Aldaba et al., in CD6, by increasing the diameter of the measured area with a new optical design. The new setup showed a similar performance when compared to the original, and the recorded images were comparable. However, the measured area was smaller than the expected theoretical diameter. Several reasons that could explain these differences were studied, including: Gaussian beam, the laser source and the incidence lens used. Changing the objective lens may be a factor to avoid he limitation in the measured diameter, and more work is to be done in this sense. Moreover, the system has been observed as being sensitive to small movements of the patient, which should also be improved in future work.

INDEX

1. INTRODUCTION

1.1 Dry Eye Disease (DED)

1.1.1 Definition

In the last years the understanding of dry eye has considerably improved, and different definitions have been published before the new one in 2017 from the Tear Film & Ocular Surface Society (TFOS), in the TFOS Dry Eye Workshop II (TDOS DEWS II) report. The earliest definitions reflected the relevance of tear film quality as well as quantity as a cause of dry eye whereas the latest led to a revised definition that focused on the clinical effects and associated signs. [1] Taking into account different important considerations, the latest definition of dry eye disease was amended by the TFOS DEWS II in 2017 to:

"Dry eye is a multifactorial disease of the ocular surface characterized by a loss of homeostasis of the tear film, and accompanied by ocular symptoms, in which tear film instability and hyperosmolarity, ocular surface inflammation and damage, and neurosensory abnormalities play etiological roles". [1]

1.1.2 Classification

An etiopathogenic classification of Dry eye disease (DED) has been set (Fig. 1) to guide diagnosis and ultimately improve patient care through appropriate treatment. However, it has also undergone different changes through the years. Two primary and separate categories were identified, aqueous-deficient dry eye and evaporative dry eye, with their corresponding sub-classifications. But, the last report presented by the TFOS DEWS, attempt to "remove any perception of exclusivity in the classification of dry eye by indicating in the scheme that aqueous deficient and evaporative dry eye diagnosis exist on a continuum rather than as separate entities". [1]

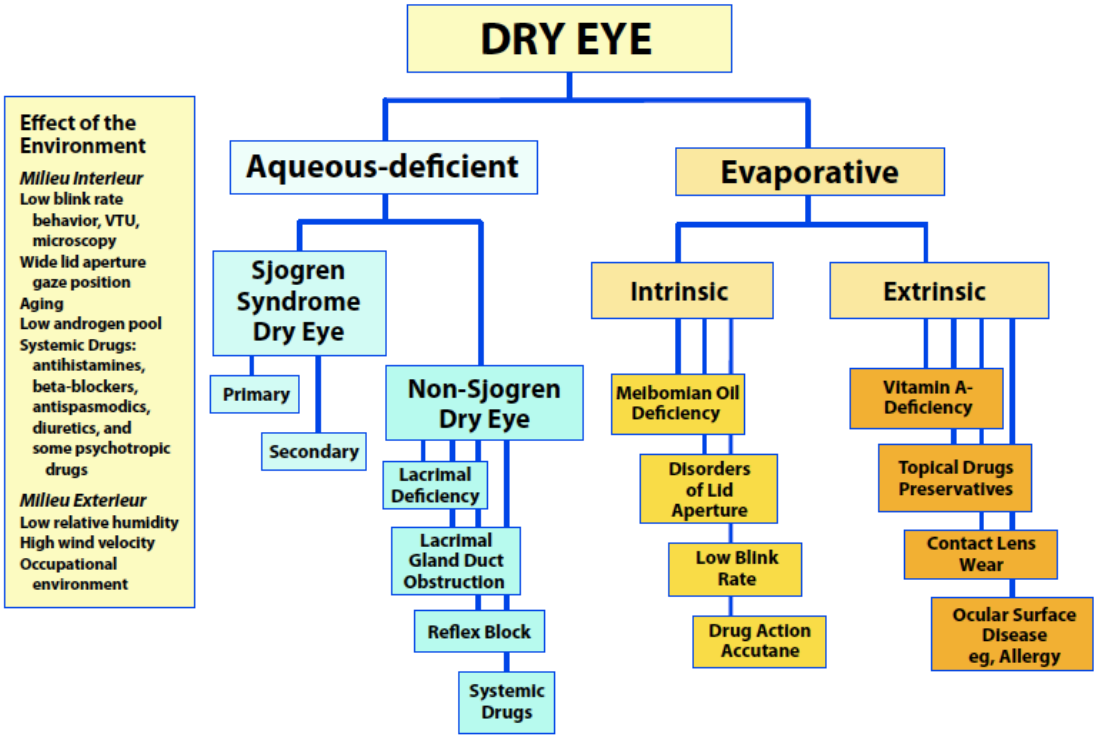

Fig. 1. Dry eye classification from the 2007 DEWS Report [2]

1.1.3 Clinical relevance

Dry eye disease (DED) is one of the most common ocular conditions. Between 5 – 30 % of patients who visit ophthalmic clinics report symptoms of dry eye. This public health problem has been growing over the past years and is becoming one of the most common conditions seen by eye care practitioners. [1,3]

Prevalence estimates for DED vary depending on the characteristics of the population studied and the diagnostic method [3]. This could be due to the limitations on diagnostic methods and the high number of existing risk factors for DED.

The most common diagnostic methods, which are going to be described in the following sections, have some disadvantages that could make DED prevalence varies considerably. Although DED diagnosis is important in the ocular health

assessment, tear film is not being tested as a significant step of a routine visual exam in clinical practices. Therefore, the methods to be used in DED diagnosis should be manageable and affordable, making it easier to be applied in clinics. Most of the used techniques on DED diagnosis have drawbacks represented by being subjective, depending on the practitioner's input, and/or invasive where there is a direct contact with the patient which could alter the ocular surface and misrepresent the results. These are considered as limitations that could affect the prevalence obtained with the different methods.

Besides the limitations in the diagnostic methods, there are several risk factors of DED, which makes it more difficult to control the results. Some risk factors that should be taken into account when diagnosing DED are: age, sex, Meibomian gland dysfunction, contact lens wear, Sjorgren syndrome, environmental exposures, refractive surgery, diabetes, etc. Detailed explanation can be found in the TFOS DEWS II epidemiology report [4]. Among all these risk factors, one of the most compelling features of DED is that it occurs more frequently in women than in men. These sex differences appear to be due to the effects of hormones, as well as other factors (e.g. genes). [5]

The above reasons can explain the variation in the DED prevalence, affected by the accuracy and reliability of certain diagnostic methods. This raises the need for objective and non-invasive diagnostic methods in an attempt for having more reliable tests to be used in clinical practice.

1.1.4 Tear Film

The tear film is the first surface of the eye that is in contact with the air and it is essential for the human eye to ensure its health and comfort. It provides the primary refracting surface for light entering the visual system as well as creating a protective and lubricated environment for the tissues of the palpebral and bulbar surfaces. [1]

Many tear film composition models had been proposed. The first one, described by Wolff, was a three-layered model, simple and logic [6,7]. But after some research it is more believed that the film structure can be described with a two-layered model with the mucous and aqueous layers forming one gel layer (mucoaqueous layer) beneath the lipid layer. The lipid layer plays an important role in maintaining stability and it is believed to reduce the rate of tear film evaporation from the cornea. The mucoaqueous layer provides lubricity and helps all the tear film to adhere to the eye. [1,2] The whole tear film thickness has been proposed to be 3 µm using reflection spectra of the precorneal tear film. [8]

The majority of the tear is secreted by the lacrimal gland, showed in figure 2, with a smaller portion secreted by the goblet cells and the accessory lacrimal glands from the conjunctiva. [1] Depending on how it is produced and why, tears have been classified into four types - basal, reflex, emotional and closed-eye, [1] where each type has different characteristics.

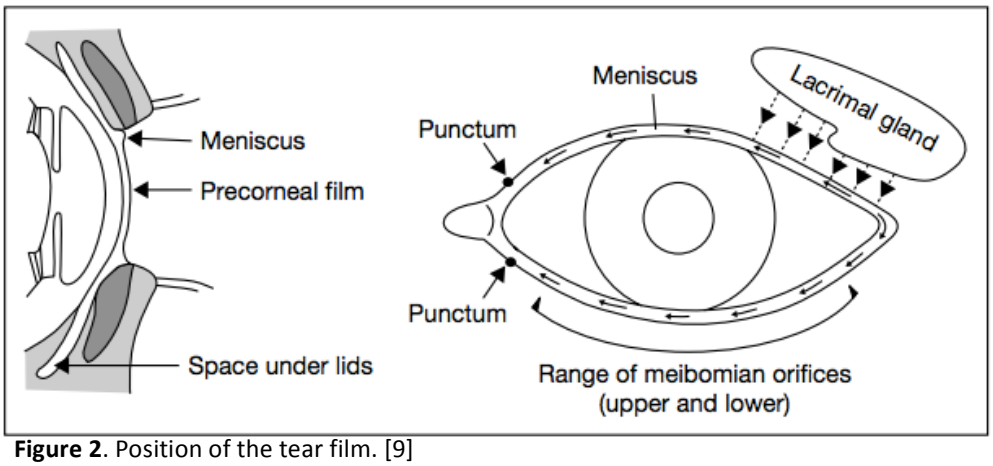

Figure 2. Position of the tear film. [9]

Tear film formation is of great interest to understand how this surface works. When the upper lid moves down over the corneal and conjunctival surface, it compresses the outer lipid layer of the tear film between the two lid edges. The outer lipid strip is compressed and probably reaches a thickness of 0.1 mm. The aqueous layer remains under the eyelids and acts as a lubricant between them

and the eyeball. When the eyelids are open, an aqueous lacrimal surface is first formed on which the compressed lipid rapidly spreads. The monomolecular lipid layer is the first to be extended followed by the distribution of the excessive lipids and the associated macromolecules are distributed on the surface of the tear film at lower speed. [10,11]

Each time someone blinks, a protective coating of tears is spread like a film over the front surface of the eye. A periodic reformation of the tear by means of blinking is necessary to maintain a continuous and healthy tear film over the pre ocular surface.

There are specific aspects regarding to the eye that are affected when dry eye occurs, therefore, they could be used for DED diagnose [12]. The main aspects are briefly discussed below:

- *Symptoms*

The symptoms and signs of DED are not directly related and vary depending on the individuals and types of DED. However, the ability to quantify ocular surface symptoms is a significant screening tool that can assist in further DED clinical evaluation. Therefore, it is recommended to administrate a validated symptom questionnaire when communicating with the patient. The most widely used questionnaire for DED clinical trials is the Ocular Surface Disease Index (OSDI), which is going to be described later. [12]

- *Visual disturbance*

Dry eye patients commonly have visual complaints that include fluctuating vision with blinking, blurred vision, glare, and eye fatigue [13]. This visual disturbance is subjectively assessed by ocular questionnaires, as the symptoms. [12]

- *Tear volume*

Tear film volume is a significant feature for ocular surface health. It can be measured with different tests as; meniscometry (tear meniscus assessment), phenol red thread test and Schirmer test, all them described in the Diagnostic Methodology report by TFOS DEWS. [12]

- *Tear film composition*

Osmolarity is the main aspect that has to be considered talking about tear film composition, which changes when dry eye occurs. Tear film osmolarity has been frequently reported as one of the best metric to diagnose and classify DED, however the actual amplitude of variation is strongly dependent on disease severity. [12]

- *Damage to ocular surface*

Patients with DED can have the ocular surface damaged in different ways. To measure how this surface is damaged there are various tests; ocular surface staining, impression cytology technique, Lid Parallel Conjunctival Folds test, *in-vivo* confocal imaging and ocular surface sensitivity test. The most appropriated diagnostic technique for ocular surface damage is the corneal staining because it shows where is the damage and the amount of it. However, it is not the most accurate one for DED diagnosis because damage in the ocular surface is not the most relevant sign for DED and it is invasive. [12]

- Inflammation of the ocular surface

Inflammation is a highlighted component on the pathophysiological mechanism of DED and has been proposed to offer a strong indicator of DED severity. However, inflammation is non-specific to DED and can occur with other ocular or systemic diseases, therefore, it is not a very reliable sign for DED diagnosis. [12]

- Eyelid aspects

Advanced DED tends to affect the eyelids; therefore to be aware of the patent's situation, it is very important to observe them before proceeding with any further measurements. But as inflammation of the ocular surface, it is not specific to this disease, and it doesn't ensure the DED diagnostic. [12]

- *Tear film stability*

Finally, impaired tear film stability has been one of the fundamental diagnostic criteria for diagnosing abnormality of the tear film as well as one of the most used techniques for DED diagnose. [14]

Tear film has its own regeneration progress that takes place after each blink during a few seconds, but then it starts to degrade and finally breaks up [14]. Although there is not accordance on how the rupture of the tear film happens, there is a general agreement about the appearance of dry spots or break ups in the tear film when blinking is prevented [15]. Moreover, the tear film layer becomes thinner when this happens [12], and the dry spots lead to height differences in this surface. And not only this but also tear film smoothness can be lost if corneal epithelium is exposed.

The time between the last complete blink and the appearance of the first dry spot is referred to as the breakup time. This is a measure of the stability of the tear film.

1.2 Methods for dry eye diagnosis

As mentioned above, there are several tests in clinical practice for dry eye diagnosis. Such as but not limited to: symptoms questionnaires, measurements of tear film stability or break up time (BUT), corneal staining technique and reflex

tear flow measure. Among these, BUT measurement is considered to be the most common technique for DED diagnosis.

Up to date, techniques for dry eye diagnose could be classified differently. On the one hand, the most widely used techniques in clinical practice can be classified in the group of conventional and traditional techniques. On the other hand, within new techniques group, some of them based on new technologies, developed over the last years, can be included. In this section, some of the conventional and new techniques are going to be briefly explained.

1.2.1 Conventional techniques for dry eye diagnose

The most used techniques for DED diagnose are characterized for being easy to use and affordable, in order to be used in clinical practise. Next, some of the most relevant ones will be discussed.

1.2.1.1 Tear Film break-up time (TBUT)

There are different ways to measure the tear film break-up time; all of them measure the interval of time that elapses between a complete blink and the appearance of the first break in the tear film.

There are two ways of how tear film break-up time measurement is performed, the invasive and the non-invasive, abbreviated as TBUT and NITBUT, respectively.

Sodium fluorescein is the product used for TBUT technique. It is instilled using either micropipette or more commonly impregnated strips, to enhance visibility of the tear film. A standardized methodology is given, ordering to blink three times and then to cease blinking until instructed. [12] While the patient ceases

blinking, the tear film is observed under a broad beam of cobalt blue illumination. A TBUT under 10 seconds is considered abnormal. [16]

This method is most commonly used in clinics due to its simplicity and affordability. However, fluorescein reduces the stability of the tear film and therefore the measurement may not be an accurate reflection of the tear film status. In addition to that, another drawback of this method is its subjectivity and the dependence on the observer's decision on when the break up occurs

Despite the drawbacks of using fluorescein to assess tear film stability, TBUT still remains one of the most commonly used diagnostic test for DED in clinical practice. [12]

In order to avoid the above mention drawbacks, some research has been done to develop non-invasive methods, such as the assessment of pre-corneal tear film BUT without the use of fluorescein (non-invasive BUT). NIBUT techniques using instruments such as the grid xeroscope or tearscope allowed an evaluation of the tear film without any physical disturbance of the film from the instillation of fluorescein and neither the possibility of reflex tearing.

However, NIBUT did not find widespread acceptance in clinical practice due to problems in quantification of tear film stability, because the results are dependent on the practitioner, which means that is still subjective. It is true that there are some of the NIBUT techniques that are not subjective; even so, they are not still widely used in clinical practise due to its cost [17]. One of the more frequently used NIBUT techniques is the videokeratography, which is going to be explained during the next sections.

1.2.1.2 Ocular Surface Disease Index (OSDI)

Among all the symptom questionnaires used to assess DED, the OSDI is the most widely used one for DED clinical trials. OSDI, figure 3, is a 12-item questionnaire designed to provide rapid assessment of the symptoms of the ocular irritation consistent with dry eye disease and their impact in vision-related functioning. It measures the frequency of ocular symptoms (3 questions), environmental triggers (3 questions) and vision related functions (6 questions). The final score reveals the severity of the patient DED. A score less than 13 mean normality. [12]

OSDI (Ocular Surface Disease Index)

Patient name: **Date of birth:** **Patient ID:**

Have you experienced any of the following during the last week?

	All of the time	Most of the time	Half of the time	Some of the time	None of the time	
1. Eyes that are sensitive to light?	☐	☐	☐	☐	☐	
2. Eyes that feel gritty?	☐	☐	☐	☐	☐	
3. Painful or sore eyes?	☐	☐	☐	☐	☐	
4. Blurred vision?	☐	☐	☐	☐	☐	
5. Poor vision?	☐	☐	☐	☐	☐	

Have you problems with your eyes limited you in performance any of the following during the last week?

	All of the time	Most of the time	Half of the time	Some of the time	None of the time	No Answer
6. Reading?	☐	☐	☐	☐	☐	☐
7. Driving at night?	☐	☐	☐	☐	☐	☐
8. Working with a computer or bank machine (ATM)?	☐	☐	☐	☐	☐	☐
9. Watching TV?	☐	☐	☐	☐	☐	☐

Have your eyes felt uncomfortable in any of the following situations during last week?

	All of the time	Most of the time	Half of the time	Some of the time	None of the time	No Answer
10. Windy conditions?	☐	☐	☐	☐	☐	☐
11. Places or areas with low humidity (very dry)?	☐	☐	☐	☐	☐	☐
12. Areas that are air conditioned?	☐	☐	☐	☐	☐	☐

Figure 3. The OSDI test by Collins Street Optometrist [18]

It has been proved by the American Medical Association that the OSDI is a valid and reliable instrument for measuring the severity of dry eye disease, and it possesses the necessary psychometric properties to be used as an end point in clinical trials. [19] However, OSDI, as all the other questionnaires, has a limitation that it is subjective and it depends on the participant´s response.

1.2.1.3 Schirmer test

This test evaluates the tear film volume, by inserting a strip of filter paper into the lower fornix of the eye and measuring the length (in mm) of wetting on the strip after a specific time.

There are two different types of the Schirmer test; Schirmer I, that measures total tear secretion (including basal and reflex) and Schirmer II, which measures the basal secretion only [20]. DED is present when the recorded scores are <10 mm and <8 mm with for Schirmer I and Schirmer II, respectively. However, using either Schirmer I or II, numerous reviews and research papers have documented high variability, low reproducibility and poor correlation with other signs and symptoms of DED [21].

All this is due to some limitations of the test; for example the testing time (5 min) which might be too long; the paper strip may not absorb as it should; it is though that there is loss of the tear due to evaporation; the test causes discomfort and there is a discrepancy for the wetting length limits in non dry-eyed patients or those with DED. [21] Therefore, it is not a very reliable test for dry eye diagnose, even though it is affordable and simple for clinical practice.

1.2.1.4 Corneal staining

Punctuate staining of the ocular surface is a feature of many ocular diseases and can be highlighted by instilling dyes, which are extensively used in the diagnosis and management of DED. Staining of the cornea occurs preferentially over its lower part, often more nasally than temporally and frequently in continuity with the bulbar conjunctival stain. The most frequently used dyes are sodium fluorescein, rose Bengal and lissamine green. [12, 22]

The three dyes act differently when instilled in the eye. Sodium fluorescein diffuses rapidly whenever viable cells experience a compromise to their integrity that is into tissues in the presence of an epithelial defect. [22] Rose Bengal stains ocular surface epithelial cells that are unprotected by mucin or glycocalyx, as well as dead or degenerated cells. And finally, lissamine green stains epithelial cells only if the cell membrane is damaged, irrespective of the presence of mucin. [22,23]

Among all dyes, rose Bengal is not clinically used because it stings on instillation and induces reflex tearing, and this modifies the results and it is uncomfortable for the patient. On the other hand, sodium fluorescein and lissamine green do not produce stinging and are well tolerated by the patients, making them the best options.

Nowadays the most used dye to observe ocular surface staining is fluorescein. It is instilled by a paper strip or by drops, and the eye has to be observed through a cobalt blue light and a yellow filter.

According to the TFOS DEWS II, corneal and conjunctival staining have been shown to be informative markers of disease severity on the severe DED; however, staining of the ocular surface in mild/moderate DED showed poor

correlation to disease severity. And although it is very economic and easy in clinical practice, it is still and invasive and subjective technique. [12]

1.2.2 New techniques

In recent years, big efforts have been made to develop objective and non-invasive methods for dry eye diagnose based on new technologies. Below is a brief description of some of the most relevant techniques.

1.2.2.1 Corneal topography

Corneal topography or videokeratography, is a non-invasive technique that maps the surface curvature of the cornea. It has been seen that corneal topography examinations help in the assessment of corneal surface irregularities in aqueous tear deficiency states.

Takashi Kojima and his research group, developed a software program called the Tear Stability Analysis System (TSAS) for the TMS-2N corneal topography instrument, in Japan. This programme takes 10 consecutive corneal topograms, as shown in figures 4 and 5, one per second for 10 seconds (see [24] for method details). Therefore, TSAS can detect subtle time-wise changes in the tear film deriving data from the distortion of the mire rings. The efficacy of the TSAS, using videokeratography as a non-invasive and an objective method of tear stability assessment, has already been established for this research group with their investigation. [24] Even though this is a complex technique and it is still in research, it has some other limitations, such as the non-measured central part of the cornea due to the characteristics of the set up. Therefore this method also has some issues that have to be solved.

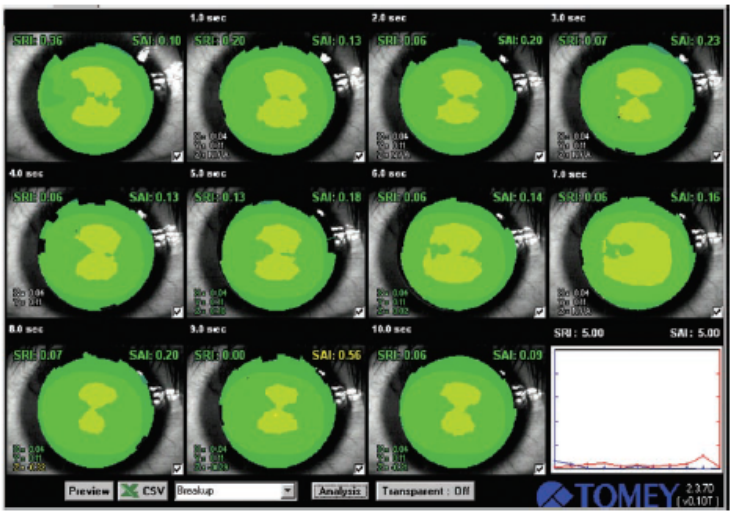

Figure 4. Representative TSAS map from a normal subject, a 38-year-old man who had a Schirmer test result of 10 mm. BUT was 12 seconds, and there was no vital staining score. [24]

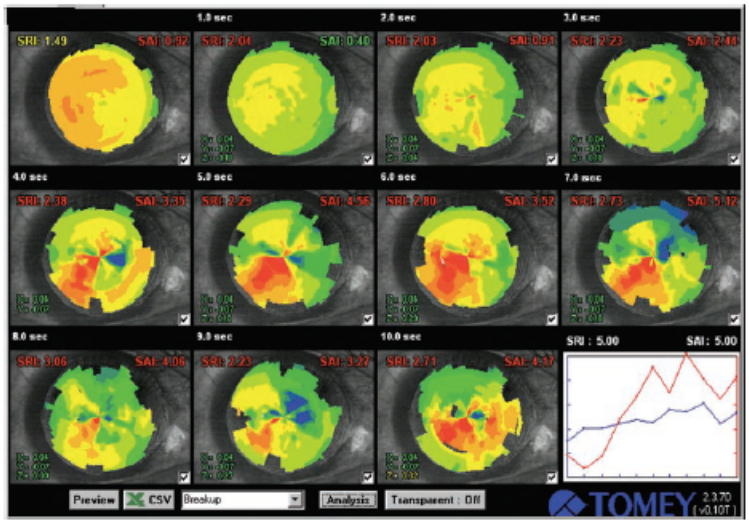

Figure 5. A representative TSAS map of a patient with dry eye, a 57- year-old man who had a Schirmer test result of 2 mm and BUT of 3 seconds. Rose bengal and fluorescein scores were both 6. Note the dramatic change in the TSAS pattern with time. [24]

1.2.2.2 Interferometry techniques

Interferometry is defined as a measurement method that uses the phenomenon of interference caused for waves to extract information [25]. There are two different interferometry techniques used for DED diagnose.

The first type uses interferometry of the lipid layer to measure tear film stability and NIBUT. The interference between light reflected from the surface of the lipid layer and from interface between that layer and the aqueous layer of the tear film, produces coloured fringes. It was suggested that these coloured patterns could be used to observe the nature, thickness and rupture of the lipid layer [26]. However, it still has some drawbacks because it only evaluates the lipid layer and not all the surface, which could lead to erroneous results [26].

The second technique is the lateral shearing interferometry. This technique has been proved to be potential for clinical applications as a non-invasive tool to study the tear topography [27]. As shown in figure 6, this technique uses a shear plate with flat optical surfaces that are normally at a slight angle to each other and with high-quality optic glass. When coherent light fall upon the plate with an angle of 45º, is reflected two times. These two reflections are quite separated due to the thickness of the plate and interference is created [28].

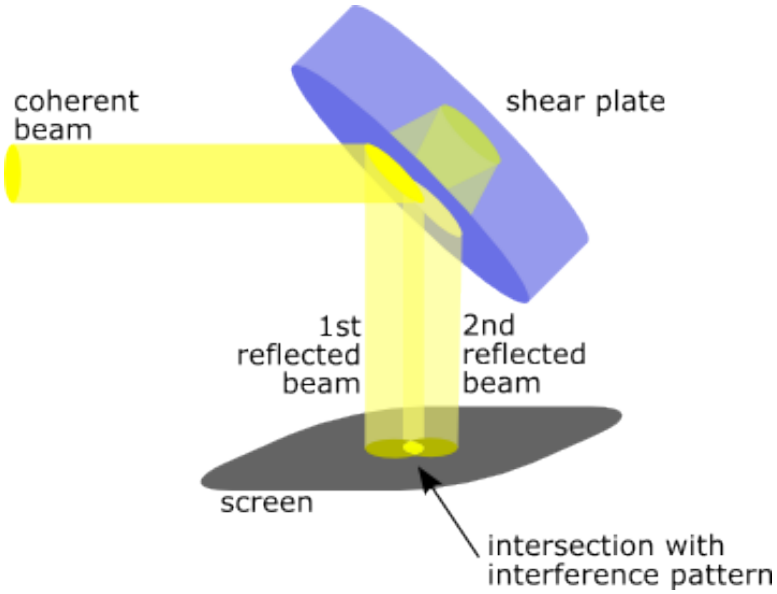

Figure 6. Principle of the shearing interferometer [28].

Although lateral shearing interferometry is one of the methods that meets the need for non-invasive testing of the tear film, and allows for precise and repeatable measurements, it still has some disadvantages. The reduced diameter and the difficulty of aligning the eye to the axis of an interferometric setup are the most important issues of the method. [17]

1.2.2.3 Optical Coherence Tomography (OCT)

Patients with dry eye disease normally have a decrease in their tear meniscus volume, and this can be measure through the tear meniscus height (TMH), as shown in figure 7. Tear meniscus variables; such as height, width, cross-sectional area, and meniscus curvature have been reported to be useful in the diagnosis of dry eye. To assess it, anterior segment optical coherence tomography (OCT) has been reported to be of high potential because of its swiftness, high resolution, and ability to provide detailed information about the ocular surface noninvasively. Due to its high resolution, this method captures Scans of the upper and lower tear menisci with a vertical beam and these are processed to obtain the THM. [29]

However, analysis of the image may be complex, time-consuming and operator-dependent, and it is not an affordable technique for clinical practise [12].

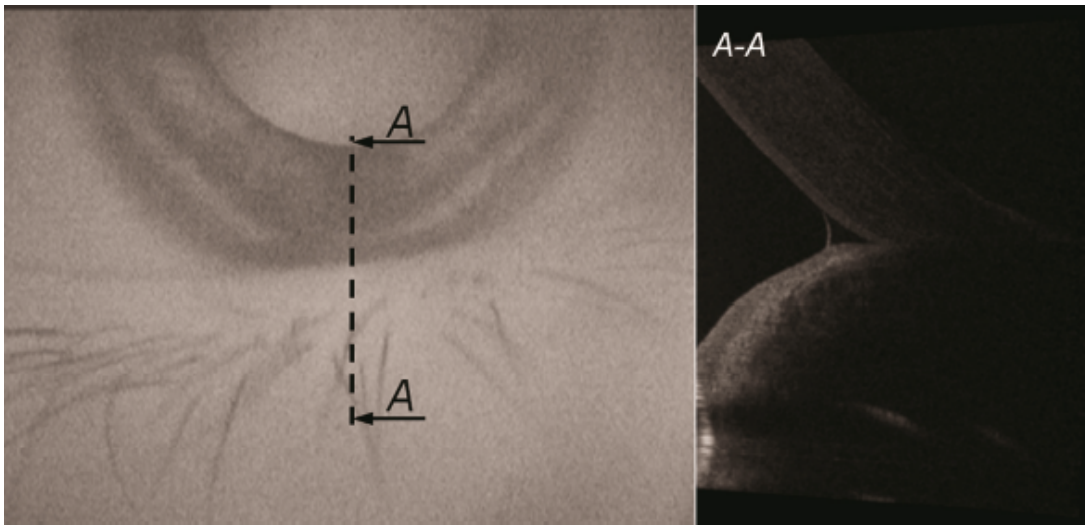

Figure 7. Bscan of the inferior meniscus. [29]

New studies [30] have been able to measure the tear film in vivo thickness and the tear film dynamics visualization using spectral domain optical coherence tomography. Their results showed that the in vivo central tear film thickness measurements are precise and repeatable with a coefficient of variation of about 0.65% and that repeatable tear film dynamics can be observed.

This approach could be used in clinical setting to study patients with dry eye disease and monitor their treatments. However, it would be necessary to acquire a larger area on the ocular surface, as the image area is limited due to the illumination pathway. Moreover, the cost of this technique is another drawback that has to be taken into account for clinical practice [30,31].

1.2.2.4 Optical quality measuring techniques

The quality of the tear film may have a significant impact on the optical quality of the retinal image. Thus, it was thought that it could be interesting to quantify tear-film quality based on dynamic analysis of retinal images. To execute these measurements, double-pass technique has been used. [32]

In double-pass technique, series of consecutive retinal images are recorded every 0.5 seconds while the patient avoids blinking. Measurements are performed under low-light conditions to naturally increase pupil diameter and maximize the method's sensitivity. From the retinal images a quality metric that measures the spread of light of the retinal image is calculated, the intensity distribution index. Then, an objective TBUT value is estimated in each eye when the intensity distribution index surpasses a defined threshold value compared with the initial baseline. [32]

Similar approaches have been proposed by means of aberrometry using Hartmann-shack technique [33].

However, these two techniques images are affected by both ocular aberrations and scattering, and not only the light coming back from the anterior surface is recorded but also all the light that comes from between the anterior surface and the retina. This means that if anything in this space is altered, the image will also be altered, and it can induce some misleading in the results [32,33].

1.2.3 Requirement of a new technique

As explained in the DEWS report, up to date, no gold standard that correlates perfectly with the dry eye diagnosis has been established [12]. Moreover, some of the methods based on new technologies cannot be adapted for clinical practise, and inexpensive and easy to use tools are needed. [34]

As explained for the CD6[1]'s research group in their work [34], dry spots appear when the tear film breaks and it can also loose its smoothness. These dry spots produce diffraction patterns when they are illuminated by coherent light due to phase differences caused by the abrupt height differences [13] of the dry spots in its surface. Therefore, and as reflected in the work done in CD6, after blinking the corneal reflex image remain without significant changes until the break up, when the image degrades [34].

First attempts made by the previous cited laboratory group in CD6, showed the potentiality of a novel method for measuring the break up time based on the interferences that appear in the corneal reflex. Although it was far from being implemented in clinical practice, it was a good point to start with.

[1] CD6 "*Center of Sensors, Instruments and Systems Development",* located in Terrassa,

1.2.3.1 Initial set up – proof of concept

The laboratory group, attempted to proof the viability of the idea that the corneal reflex image is degraded when dry spots appear with a first set up, and thus this one could be used to measure the break up time.

The initial set up included a collimated laser (λ=780nm) projected to the cornea after reflection on a beam-splitter. The reflected light was registered in a CCD camera after passing through the beam-splitter and a focusing lens. (Figure 8)

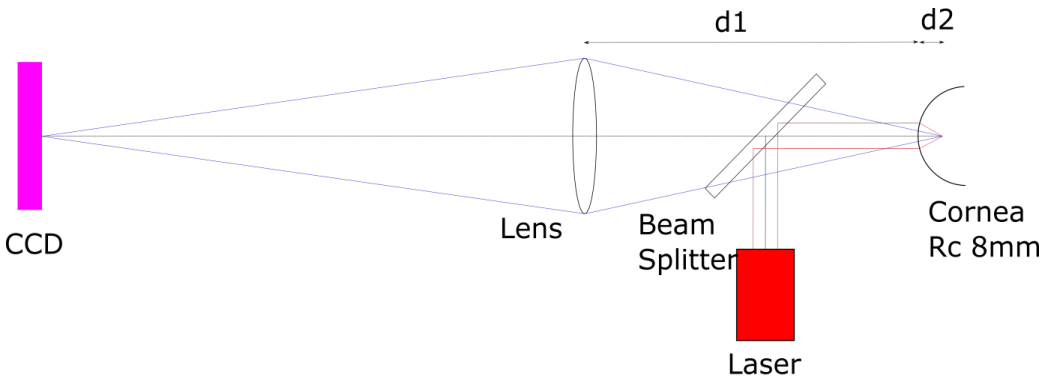

Figure 8. Schematic representation of the initial set up used for the proof of the concept of the idea.

The set up was built and some measurements were taken to proof the concept. It was seen that the corneal reflex image quality depended on the tear film quality, which meant that after blinking, when the tear film was a smooth surface, there was a regular image, similar to a PSF[2]. Contrary, when blinking was prevented and the tear film degraded, so did the corneal reflex image, as consequence of the interferences caused (diffraction, phase difference and speckle) by the dry spots. (Figure 9)

[2] The **point-spread function** (**PSF**) describes the response of an imaging system to a point source or point object.

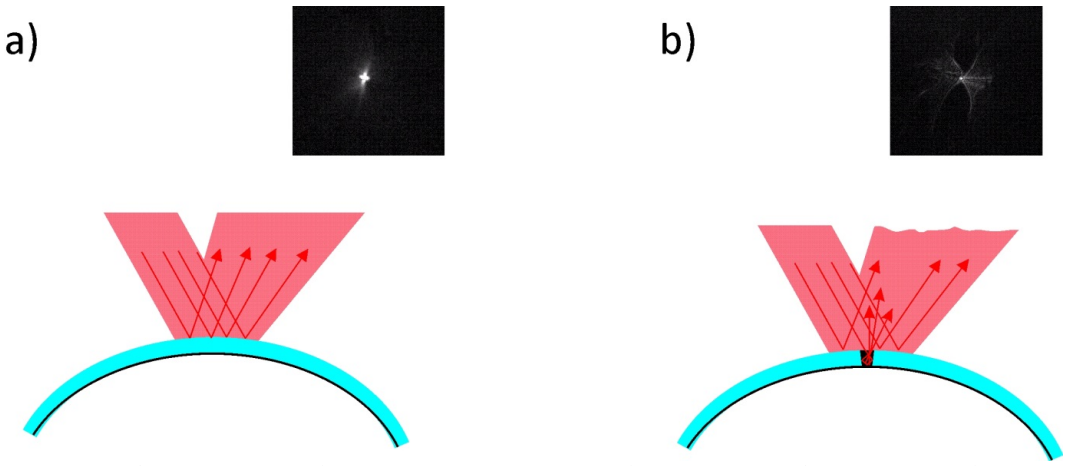

Figure 9. a) Post-blink tear film and recorded corneal reflex image and b) break up tear film and recorded corneal reflex image.

With these results, it could be proved the potentiality of the idea to measure tear film dynamics and more specifically tear film break-up time in an objective and non-invasive manner. However, the setup had a main drawback: the diameter of the measured area was small, more specifically was: 1.69mm.

With this diameter the clinical application of the measurements would be limited, because the eye is big compared with this diameter, thus the tear film could broke somewhere else of the eye.

In the figure 10 a detailed schematic representation of the measured areas is shown for the conditions of the initial setup.

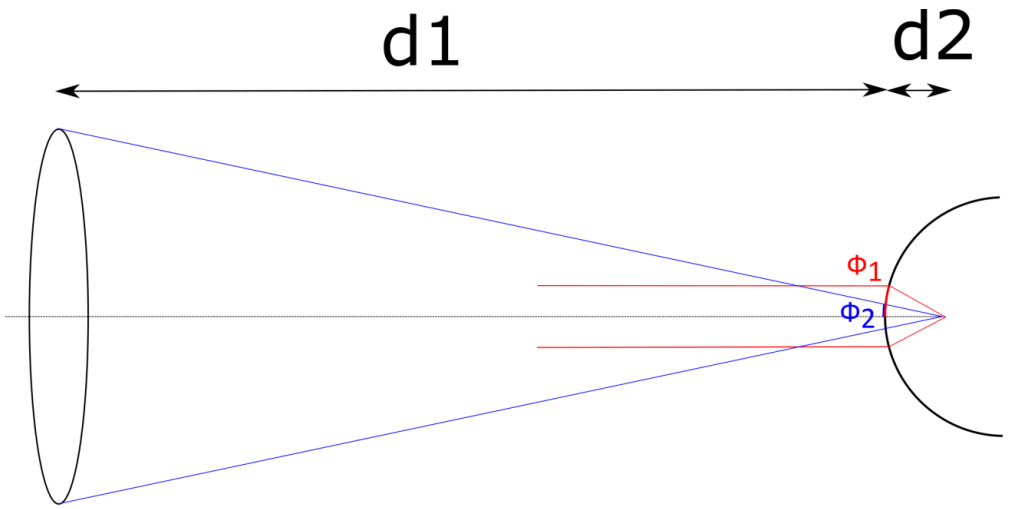

Figure 10. Incidence (red) and reflected (blue) light.

The scheme shows also how the light acts. In red is represented the incidence light, which was collimated and it reached the eye. The reflected light is shown in blue. As the incident light was collimated, the image of this light was formed at its focal distance (f'= -R/2=-4mm). Thus, light emerging from this point passed through the lens. The measured area could be determined by:

- Incident light: The diameter of the laser beam (Φ_1).
- Reflected light: The angle subtended by the diameter of the lens and the distance d1+d2 (Φ_2). The corneal area inside this angle could correspond to the measured area.

The smallest of both areas (Φ_1 or Φ_2) determined the final measured area. In the specific case of this setup the specifications were as follows:

- Lens: f'=50mm and Φ25mm.
- Incident laser beam: 4mm (could be increased to 10mm)
- D1=55mm
- D2=4mm

With this data, the diameter of the measured area can be calculated and it corresponded to:

$\Phi_1 \rightarrow \Phi_1$ = 4mm. This one could be increased to 10mm

$$\Phi_2 \rightarrow \frac{\Phi \text{ lens}}{(d1+d2)} = \frac{\Phi_2}{d2} \rightarrow \Phi_2 = \frac{\Phi \text{lens}}{(d1+d2)\times d2} = 1.69mm$$

The results showed that $\Phi_1 > \Phi_2$, therefore the diameter of the measured area was 1.69mm. Thus, the team intended to find a way of improving the measured area.

1.2.3.2 Second set up

The laboratory group continued searching what could be done to improve the diameter, and they found three different options:

1. Increasing the diameter of the lens
2. Decreasing the "d1" distance, which implies decreasing the focal length.
3. Changing incidence vergence.

To combine the two first ways in a new setup was decided; therefore, it was constructed with a larger diameter of the lens and a shorter focal length. But those changes involved some limitations. It was not possible to have a large diameter lens with a short focal length, for example a lens with Φ=75mm and a f'=25mm. It is only possible to have lenses with equal focal length and diameter, and the possibilities were the ones in table 1.

Lens Φ (mm)[3]	f' (mm)	Φ effective (mm)[4]
73	75	3.69
48	50	3.55
38	40	3.45
23	25	3.17

Table 1. Possible lenses that could be used.

Finally, it was decided to use a f'=50mm and Φ=50mm from Edmund (#32-970), specifications shown in table 2:

Lens Φ (mm)[3]	f' (mm)	Dist_lens_eye (mm)	Φ effective (mm)[4]
49	50	44	4.08

Table 2. Characteristics of the chosen lens.

[3] Lens diameter minus 1mm for lens holding
[4] Effective diameter that would correspond to the measured area

Besides the lens, there were more changes in the second setup. Firstly, as it is shown in figure 11, the beam splitter was removed and there were changes on the position of the elements. The light source, located on the temporal side of the left eye with an incidence angle of 27 degrees relative to the optical axis of the eye, it consisted of an infrared laser diode (λ = 780 nm) coupled to an optical fibre and collimated. The light, after being reflected on the tear film, goes through a lens (L1) with a focal length of 50 mm and a diameter of 50 mm, and then recorded using a CCD camera (CCD 1). The images seen on the CCD 1 were defocused 1 dioptre, in order to easily detect the changes in corneal reflex images. An auxiliary camera CCD was used for pupil monitoring and centring the patient (CCD 2). [34]

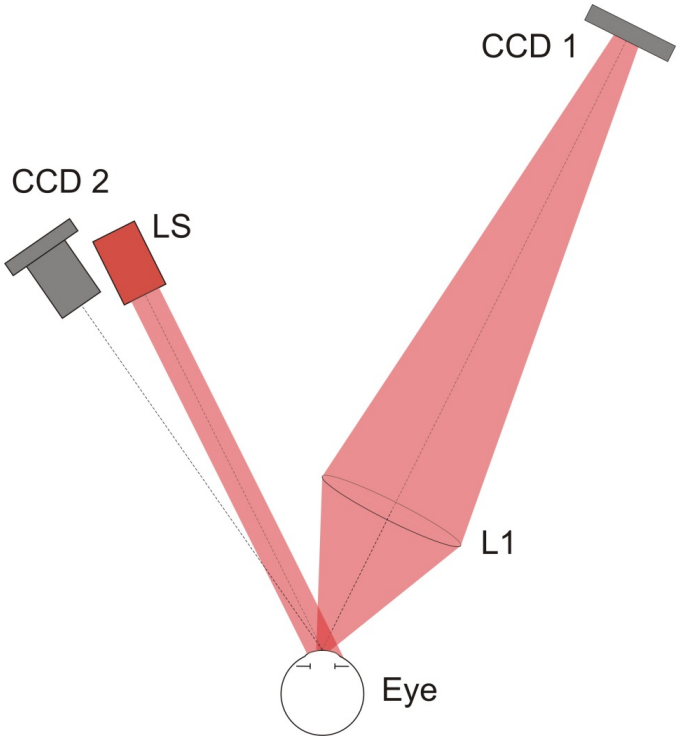

Figure 11. Schematic diagram of the proposed setup. LS: light source, L1: lens, CCD 1 and CCD 2: CCD cameras [34].

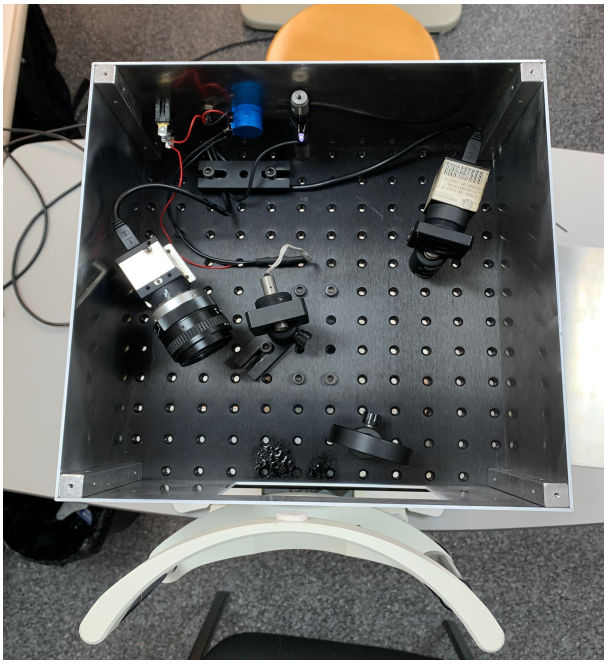

Figure 12. Second setup build at the optical bench.

With the built setup, seen in figure 12, it was proved that this setup allowed taking measurements in an area of 3.70 mm. Thus, it permitted the research group to record some images of the effect of break up on corneal reflex images as shown in figure 13.

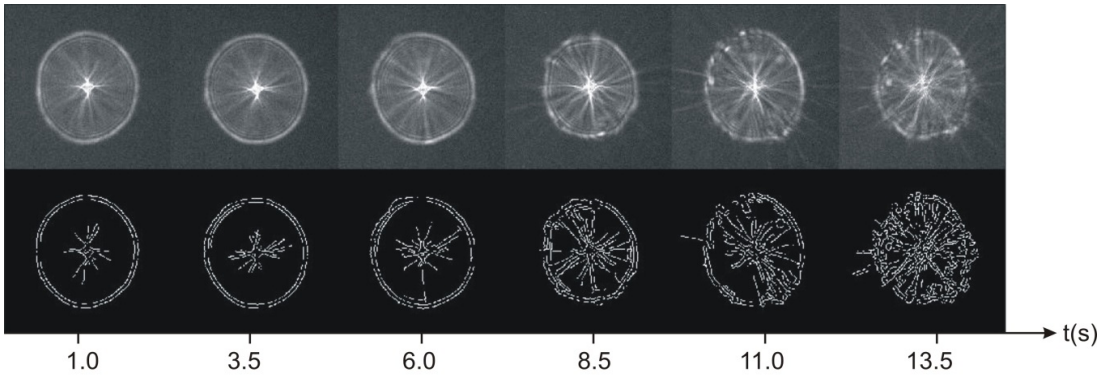

Figure 13. Corneal reflex image degradation when blinking is prevented [34].

An image processing was required in order to objectively determine the occurrence of such break ups. Among all the different methods that could be used for it, it was agreed, due to its simplicity, to count the number of the structures in which the image was broken as a result of the appearing dry sports.

For this purpose, the image was binarized (Figure 13) and the structures were detected using Matlab software and its image toolbox (MathWorks Inc., 2015). [34]

The number of counted structures was plotted against time and an exponential curve was fitted, as seen in figure 14. When the tear film was stable, the corneal reflex image remained the same and the number of counted structures was almost equal. Nevertheless, at the moment of the brake up, the corneal reflex image was degraded and the number of structures increased dramatically. For this reason, the BUT was assigned to the moment when the number of structures rose up, which corresponded with the end of the horizontal asymptote of the fitted curved. This point was automatically identified by a Matlab routine designed for this purpose. [34]

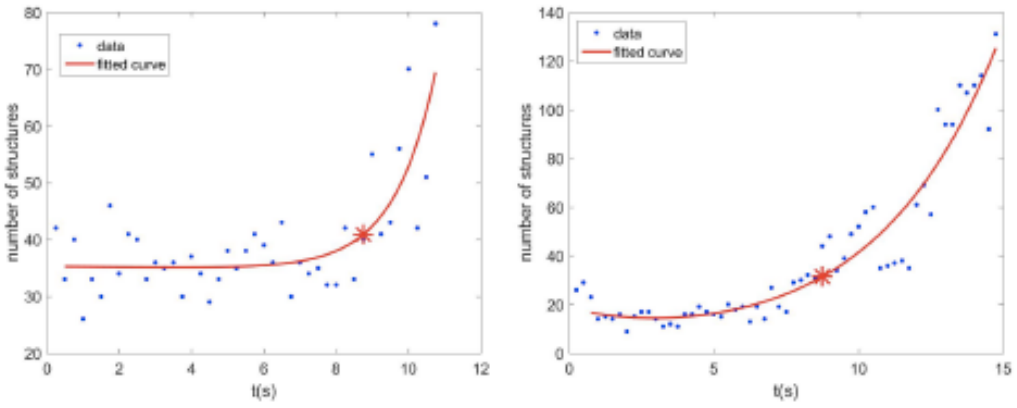

Figure 14. Number of structures counted plotted against time after blinking for different participants. Experimental data is plotted with blue dots, the fitted curve in red, and the break up time with a red asterisk. [34]

The images obtained with the experimental setup were reproduced in simulations using Matlab, such as the ones in figure 15, trying to recreate the most real situation of what was happening on the cornea. In the presence of break up, the light reflected by the surface was simulated as a beam with constant amplitude and local phase variations at the location of the breaks up,

creating structures of 0,2mm in diameter and 2.50±0.15nm deep and distributed randomly along the pupil. With methodology described in reference [34], the amplitude and the phase at the observation plane were computed, and with this simulations it could be seen the behaviour of the light under the presence of break ups. The results were comparable to the real corneal reflex images. [34]

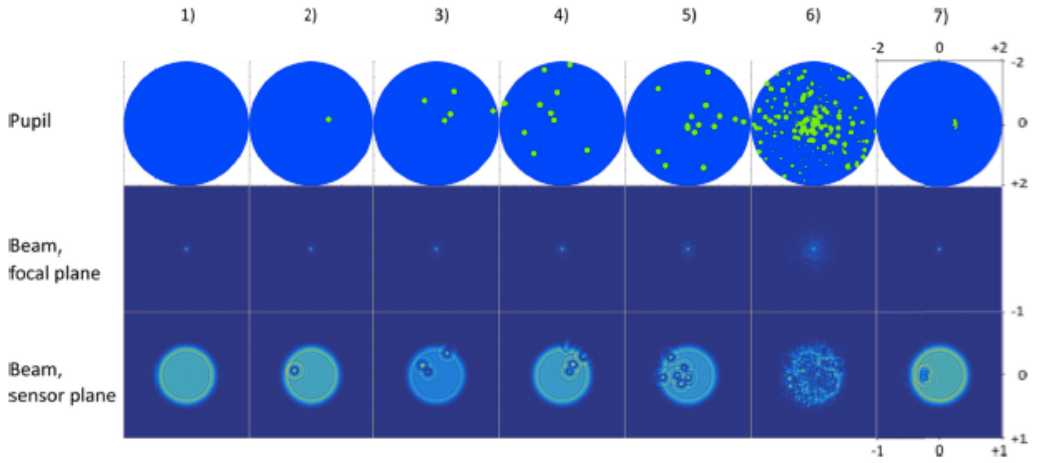

Figure 15. Simulations of the tear film break up created with Matlab. [34]

In the first line of figure 15, dry spots in the measured area were simulated, from 0 to a lot of them. In the second line, the focused beam was simulated to see how the image was and also compared to the third line where the beam was defocused. As expected, the corneal reflex images degradation was proportional to the number of breaks up simulated, even though the simulation had some differences from the real situation. And it was also confirmed that it was easier to observe these changes with a defocused imaged rather than with a focused image [34].

Besides measuring the NIBUT with the proposed method, it was also measured and compared with TBUT technique using fluorescein. After all the measurements, it was found a mean difference between both methods, of 4,08 seconds, with shorter break up times for the TBUT method.

Although the research group showed the suitability of a new objective and non-invasive method for measuring tear film breaks up, the reduced area still was a limitation. [34] This drawback was due to the fact that it was seen that the tear film was commonly broken from the periphery [35]; therefore, the measured area was still not enough and it was thought that this could be overcome with a new design of the optical setup.

All in all, it has been seen that DED is one of the most frequently encountered ocular conditions. Although it is clear that DED prevalence is high, it still has significant fluctuations, mostly due to the limitations of the conventional diagnostic methods used in clinical practice [3]. The most relevant drawbacks of these techniques are the subjectivity and the invasive method. Therefore, some new objective and non-invasive techniques based in new technologies have been developed, but they cannot be adapted for clinical practice particularly due to their cost. Recently a new inexpensive and easy to use tool, which was meant to measure the NIBUT, was developed at CD6 in order to guarantee a new effective technique for DED diagnose. However, this new technique presented a limitation on its measured area [34]. The diameter of this area is small while the tear film commonly breaks from the periphery [35] For all this reasons, the aim of this work is to improve the previously mentioned setup developed by Aldaba *et al.* in CD6, in order to increase the diameter of the measured area by changing the design of the setup.

2. METHODOLOGY

The application of the second setup in clinical environment highlighted the capability of the method for measuring the break up time in daily clinic (due to being simple and easy to use), but also showed a drawback due to the measured area. The almost 4mm of diameter of measured area were insufficient for dry eye diagnosis, mainly due to the appearance of the first dry spots in the peripheral area rather than in the center. Thus, in this section the tentative procedure to improve the setup, in order to extend as much as possible the measured area, is going to be described.

2.1 New setup drawing

As referred in the previous section, the first attempt for increasing the exposed area consisted on shorter focal length and larger diameter, but showed limited results (almost 4mm of diameter). To solve the diameter problem, a change in the incidence vergence is proposed in the new set up.

When the incidence vergence of the laser is changed, the image is created in a different position (different from f' in the first setups) and thus the corneal exposed area is different. In figure 16, two different incidences are shown; the incidence of a collimated light (left) and near distance incidence (right). As can be seen, the measured area (smallest diameter) is different in both cases.

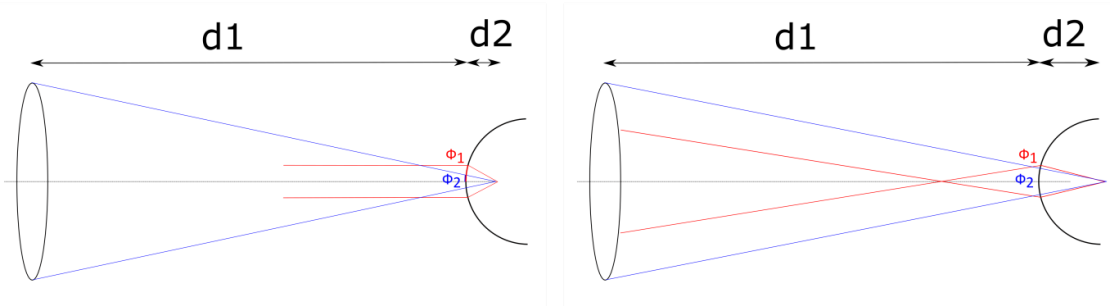

Figure 16. Incidence (red) and reflected light for collimated incident light (left) and near incidence (right).

From the different combinations of laser incidence, the one that maximizes the measured area is the one that places the lens with its focal plane at the center of curvature of the cornea so that the incident beam is normal to the tear surface. This is a similar configuration to those proposed by Licznerski [36] and Dubra [27], and enables obtaining a measured area with a larger diameter. For all these reasons, a setup with normal incident beam is proposed.

The easiest way to calculate the approximate diameter is triangulating, as in figure 17. It is known that the incidence lens has a f'=50mm and a Φ=50mm (49mm for the lens holding), and a mean corneal radius of curvature of 8mm. Therefore, the distance from the image formation to principal plane of the lens is 50mm and 8mm from the image formation plane to the corneal plane, in order to have the previous explained properties. Thus triangulating, the exposed area diameter is over 8mm.

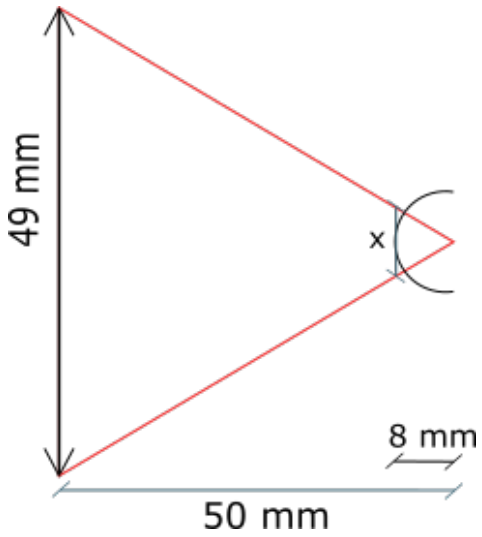

Figure 17. Triangulation to know the theoretical measured area.

2.2 Material & Setup

The proposed setup includes different specific material, which is going to be described below. As it can be seen in figure 18, the setup consists of a laser as the light source, a collimating lens, a beam splitter, an incidence lens, a focusing lens and a CCD camera.

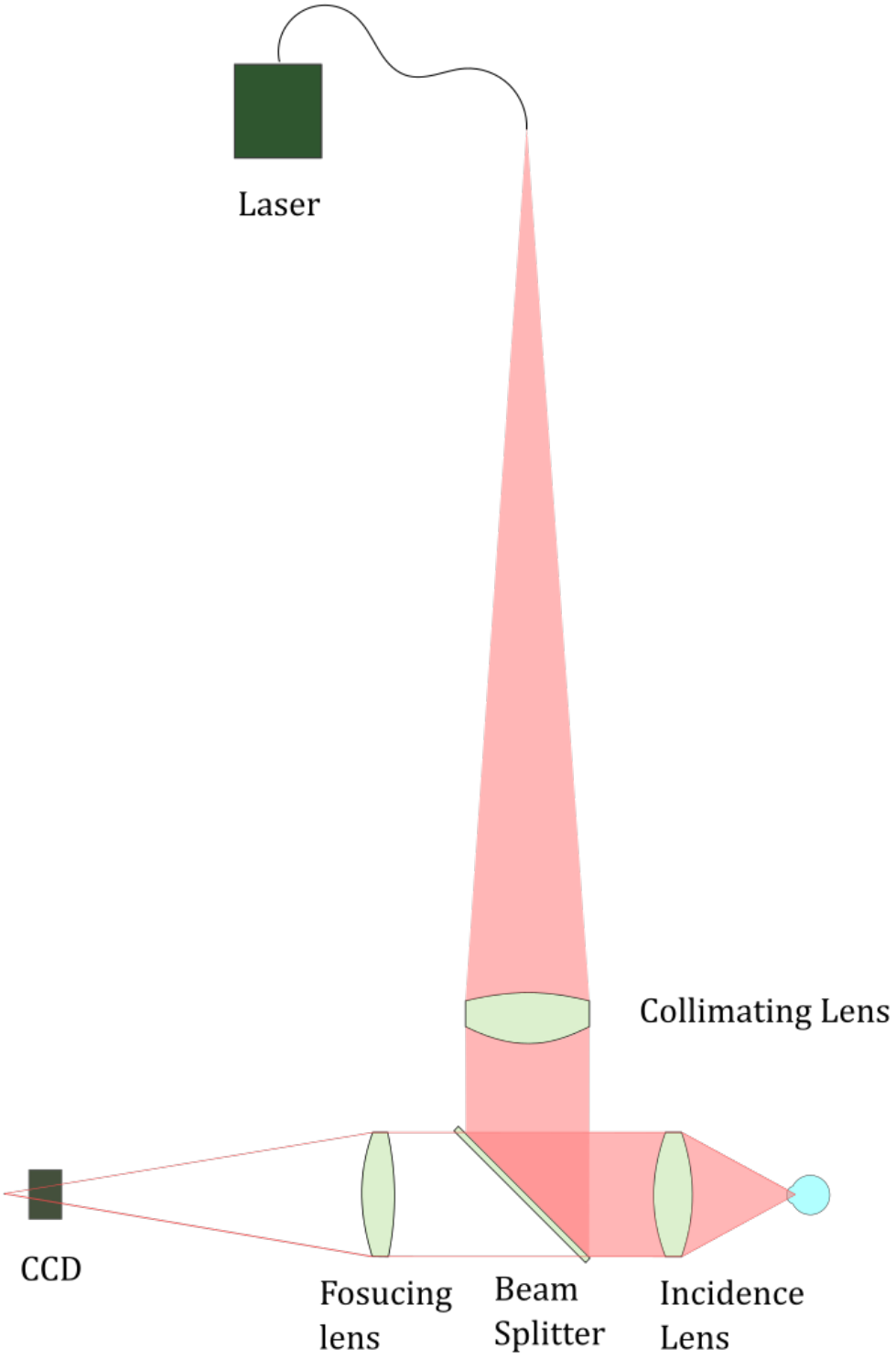

Figure 18. Optical scheme of the proposed setup at scale 1:3.

- *Light source*

It consists of a fibre laser named MC7805MC from Monocrom. Its most relevant characteristics are the ones in table 3:

Wavelength	780 nm
Electric current	60 mA
Power	1.5mW

Table 3. Fibre laser features.

- *Collimating lens*

It is a lens from Edmund optics, reference #31402 [37]. As it is specified in Edmund Optics page, the most relevant specifications of the lens are the ones in table 4 and also shown in figure 19:

Diameter (mm)	63.59 +0.00/-0.10	**Effective focal length EFL (mm)**	354.87
Center thickness CT 1 (mm)	11.94	**Back focal length BFL (mm)**	344.52
Center thickened CT 2 (mm)	8.86	**Edge thickness ET (mm)**	17.43
Numeric Aperture NA	0.09	**Wavelength range (nm)**	400 - 700

Table 4. Collimating lens features.

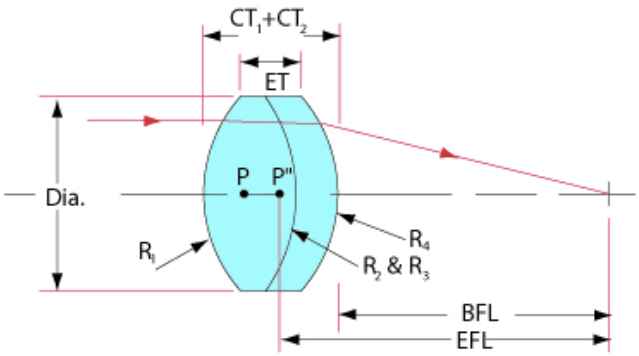

Figure 19. Technical image showing some properties of the used collimating lens. [37]

- *Beam splitter*

It is a beam splitter from Edmund Optics, reference #4890 [37]. As it is specified in Edmund Optics page, the most relevant specifications of the beam splitter are the ones in table 5 and also shown in figure 20:

Dimensions (mm)	75.0 x 75.0	**Angle of incidence (º)**	45
Reflection/transmission Ratio (R/T)	50/50	**Thickness (mm)**	3
Clear aperture (%)	>85	**Wavelength range (nm)**	700 - 1100

Table 5. Beam splitter features.

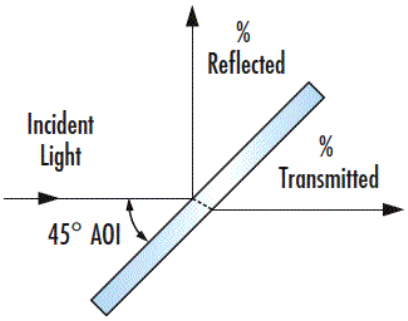

Figure 20. Technical image showing some properties of the used beam splitter. [37]

- *Incidence lens*

It is a lens from Edmund optics, reference #32978 [37]. As it is specified in Edmund Optics page, the most relevant specifications of the lens are the following ones in table 6 and also shown in figure 21:

Diameter (mm)	50.00 +0.00/-0.025	**Effective focal length EFL (mm)**	50.00
Center thickness CT (mm)	16	**Back focal length BFL (mm)**	45.30
Edge thickness ET (mm)	7.39	**Wavelength range (nm)**	400 - 2500
Numeric Aperture NA	0.50	**Clear aperture CA (mm)**	49

Figure 6. Incidence lens features.

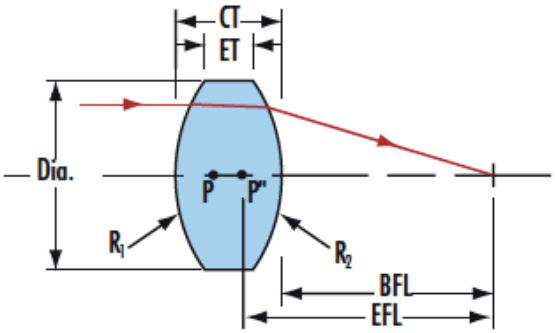

Figure 21. Technical image showing some properties of the used incidence lens. [37]

- *Focusing lens*

It is a lens from Edmund optics, reference #49391 [37]. As it is specified in Edmund Optics page, the most relevant specifications of the lens are the ones in table 7 and also shown in figure 22:

Diameter (mm)	50 +0.00/-0.025	**Effective focal length EFL (mm)**	150
Center thickness CT 1 (mm)	9.50	**Back focal length BFL (mm)**	147.17
Center thickened CT 2 (mm)	4	**Edge thickness ET (mm)**	8.92
Numeric Aperture NA	0.17	**Wavelength range (nm)**	400 - 1000

Figure 7. Focusing lens features.

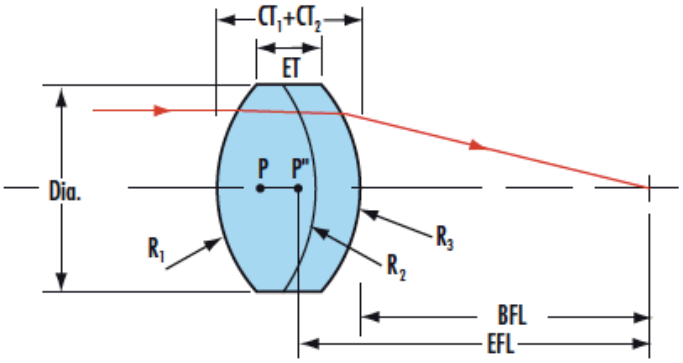

Figure 22. Technical image showing some properties of the used focusing lens. [37]

- *CCD camera*

The CCD camera, the one in figure 23, used is from IDS Imaging development Systems [38], and its reference is UI-1240LE-NIR-GL (AB00189). The most relevant specifications of the camera are the ones from the sensor, and they are the ones in table 8:

Sensor type	CMOS mono	**Optical size**	6.784 mm x 5.427 mm
Resolution	1.31 Mpix	**Pixel size**	5.3 µm
Resolution (h x v)	1280 x 1024 pixel	**Readout mode**	Progressive scan

Table 8. CCD camera features.

Figure 23. CCD camera used in the new setup. [38]

The described material is the one that was going to be used to build the new setup. Within this configuration, the light, figure 15, emerges from the fibre laser (λ=780nm), which is situated at 344.52 mm (BFL) from the back surface of the collimating lens. Once the beam is collimated, it reaches to the beam splitter. The BS is placed with an angle of 45º, relative to the axis of the beam, in order to reflex the light with an angle of 90º towards the incidence lens. As a consequence of this configuration, the beam is collimated and well centred to the incidence lens, the one with an EFL of 50mm. After passing through the lens, the beam focuses at the EFL, which is 50 mm, where the centre of curvature of the patients eye is situated. The cornea acts like a mirror, therefore, the light goes out the same way as it has entered, and it collimates again after the

incidence lens. Being collimated passes across the BS and reaches to the focusing lens, where the beam focuses at its EFL that is 150mm.

Finally, there is the CCD camera settled closer than the EFL in order to have the image defocused, as in the previous setups [34]. The images are better defocused because any change in them is easier to detect. The programme called Ueye Cockfit 2.48.000 has been used to take some images, record videos and also help in the alignment of the setup.

3. RESULTS

3.1 General results

When each of the elements was at its precise position, as seen in figure 24, to record some images with an artificial eye was possible. These images, one of them showed in figure 25, were compared with the ones obtained in the previous work done by Aldaba *et al.* [34] to prove that they were similar and thus, correct.

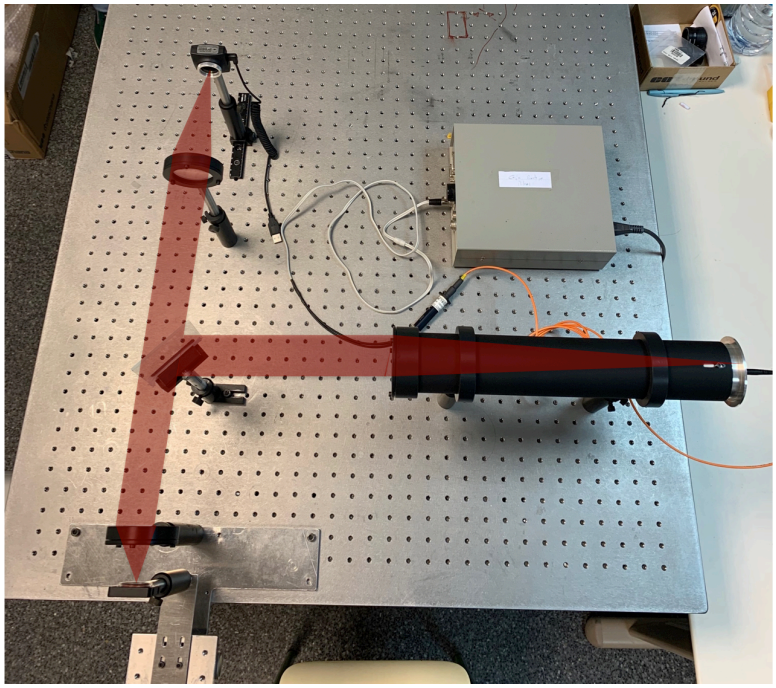

Figure 24. New setup build at the optical bench.

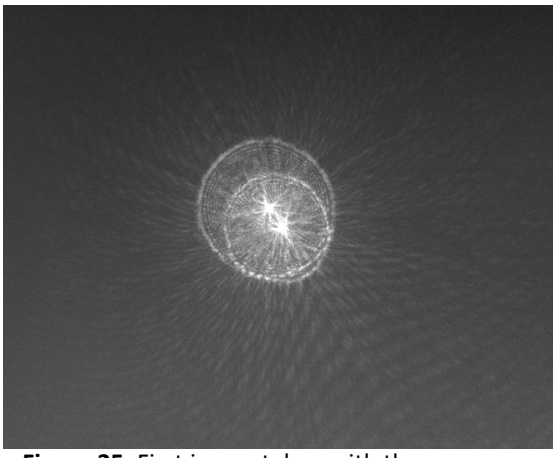

Figure 25. First image taken with the new setup.

Therefore, observing the obtained images, similarities between the ones taken in the previous research and the new ones were found. That meant that the technique was apparently working as it had to.

In figure 25, it can be observed that there are two circular images, one in front of the other. This is due to the distance between the two surfaces of the artificial eye, which gives an image for each of the surfaces. In the real eye, this distance corresponds to the corneal thickness, and although it can be different between people, it is generally really thin, around 0.535 µm [39]. Moreover, the material after the cornea is not air, but aqueous humour, and this reduces the difference between their refractive indexes, being 1,376 in the cornea and 1,336 in the humour vitreous [40]. These two characteristics leads to only have one visible image when a real eye is measured, not as with the artificial eye. For instance, in figure 26, it can be seen the double image created by the two surfaces of the artificial cornea. The front surface, where tear film break up time has to be observed, is the biggest image, where the contact lens is lies on.

In order to see if there is degradation of the registered corneal reflex image, a sequence of images with a contact lens on the artificial eye was recorded during a minute. In figure 26, images corresponding to just after the insertion of the contact lens (left) and one minute after (right) are shown. As it can be seen, at the beginning the image was clear, but almost one minute later, it could be seen that as the contact lens dewetted the image degraded.

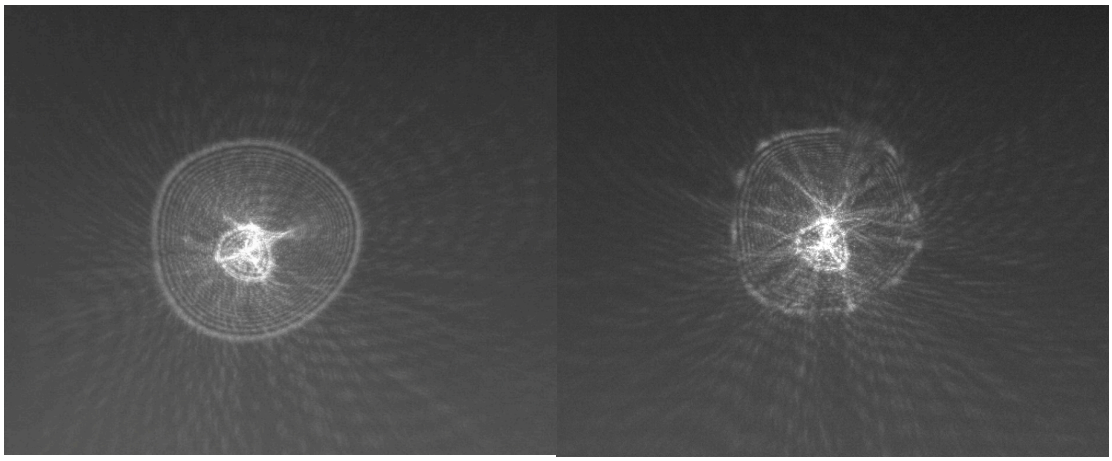

Figure 26. Image with a contact lens on the artificial eye after the insertion (left). Image with a contact lens on the artificial eye almost one minute after the insertion (right).

These first results showed that the setup was properly working. Therefore, the next step was to prove that the measured area had the diameter that should have, 8 mm as seen in methodology.

3.2 Measured area

As previously explained, to obtain the largest diameter of the measured area, the beam has to be focused at the centre of curvature of the cornea, as proposed by Licznerski [36] and Dubra [27], so that the incident beam is normal to the tear surface. This means that the cornea has to be placed at 8 mm ahead of the focusing point of the lens, therefore is where the measured area was calculated.

Firstly, it was thought on confirming the 8 mm diameter by putting different diaphragms in front of the artificial eye, starting with one of 10 mm of diameter centred in front of the artificial eye and reducing it until any change in the image appears. This different pattern would indicate that the measured area is slightly larger than the diameter of the diaphragm that has changed the image.

Nevertheless, with the diaphragms, it was seen that the image wasn't changing until placing a diameter of over 3 mm. This could mean that either the setup

wasn't working as it had to due to some problem in it, or that the method for calculating the measured area wasn't the appropriate one. Thus, it was decided to use the camera sensor to calculate how the diameter of the beam was changing with the distance after the incidence lens. This process was designed to determine the validity of the practice with respect to the theory. If the diameter of the beam was 8mm, at an 8mm distance, from the lens the practice would concur with the theory.

The camera without its lens assembly was settled at the focus of the incidence lens and moved closer to it in 1mm steps. In each position the diameter of the light beam at the sensor was measured. With the uEye programme the number of pixels could be counted. And as the resolution of the camera was known, 5.3 µm x pixel [38], it was possible to measure the size of the image with this formula:

$$Diameter\ (mm) = \frac{Nºpixels \times 5.3}{1000}$$

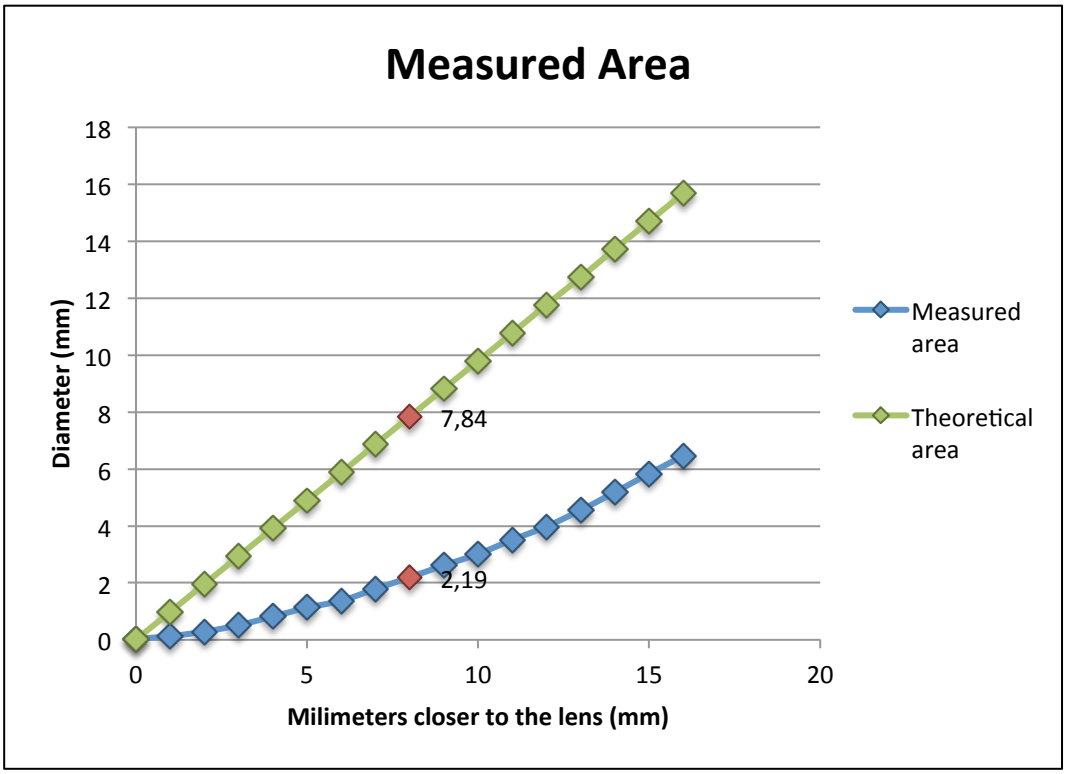

Figure 27. The graphs plots the diameter obtained if the distance between the lens and the camera decreases.

In figure 27 the measured diameter of the light beam for each position of the sensor is shown. In blue, the measured diameter is shown; in green the theoretical diameter is plotted. The red mark corresponds to the position of the cornea in the proposed setup.

As can be seen, there are noticeable differences between the measured and the theoretical area. For example, for the specific position of 8mm, the corneal plane, the theoretical area is of 7.84mm while the real measured area is of 2.19mm. To confirm the results, this process was done more than one time, but no changes were appreciated.

After discussing the problem with CD6 staff it was hypothesized that it could be due to the following reasons: the Gaussian distribution of the beam, the laser itself or the incidence lens.

- *Gaussian beam*

Most of the lasers have the same specific propagation characteristic. In general, they emit beams with a Gaussian intensity profile, seen in figure 28 and 29. In these cases, it is said that the laser is operating in the fundamental transverse mode, or "TEM_{00} mode" [41].

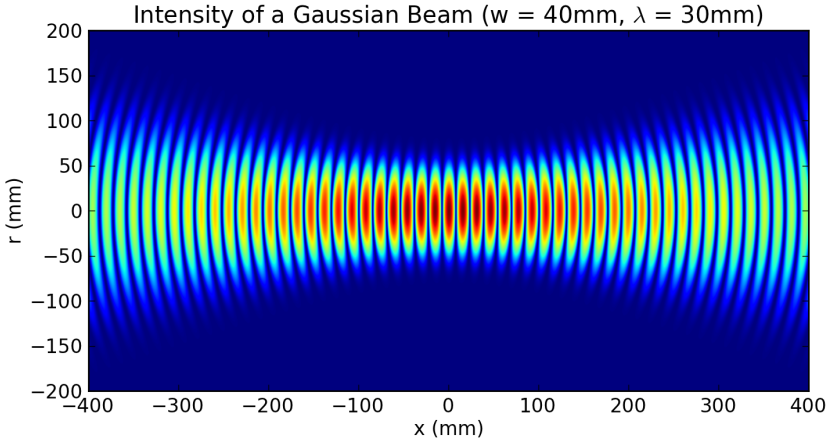

Figure 28. Intensity of a simulated Gaussian beam around focus (x = 0) at an instant time [41].

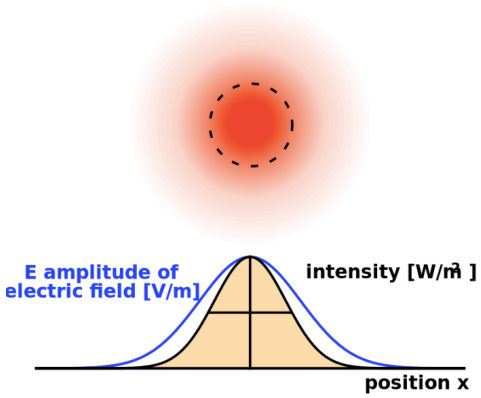

Figure 29. Top: Transvers intensity profile of a Gaussian beam. Black curve: Intensity in radial position from the beam axis [41].

When a beam passes through a lens, its characteristics change depending on the lens features, but it still has a Gaussian profile. Therefore, this distribution could affect the measured area decreasing it. To confirm that this was the problem and, moreover, to solve it, a new system in the setup was incorporated. This new part of the setup consisted in focusing the laser by means of a short focal length lens, where a diffusor was attached, and then filtered with a pinhole of 100µm, only letting pass the central part of the beam, which is the most intense and avoiding the intensity decrease at the peripheral parts.

With this new configuration, the diameter of the beam after the incidence lens was measured again, and the results were plotted in the following graph in figure 30. In this graph, the theoretical diameters were calculated by triangulation, the Gaussian beam was not taken into account.

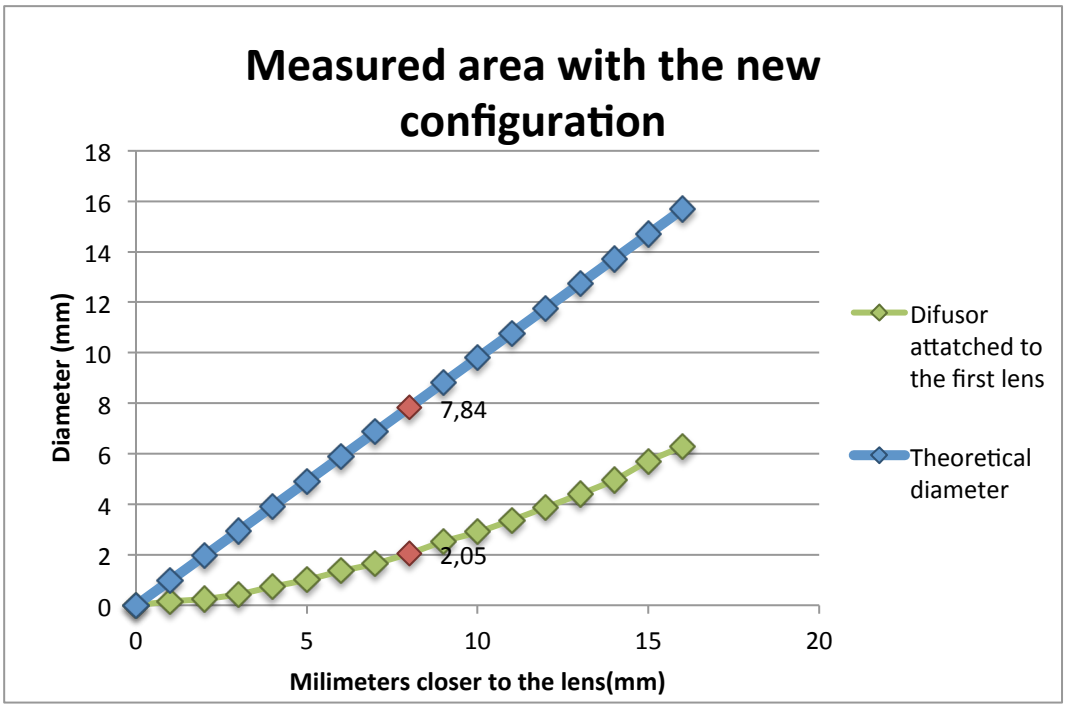

Figure 30. The graphs plots the diameter obtained incorporating a pinhole and a diffusor if the distance between the lens and the camera decreases.

As the graph shows, the measured diameter was almost the same as without the new configuration. That could mean either the pinhole wasn't improving the intensity distribution of the beam, or that the Gaussian beam distribution was not affecting the measured area. To prove what was really happening, the theoretical Gaussian beam waist was calculated, counting on Ana Rodriguez's helps, a CD6's member.

The equation that allows us to find the beam waist diameter (w_0) in terms of the input parameter, this means the diameter when the beam is focused (x=0), is the following one [42]:

$$2w_0 = \left(\frac{4\lambda}{\pi}\right) \times \left(\frac{F}{D}\right)$$

λ being the wavelength of the laser, F being the focal of the lens and D being the diameter of the lens.

Knowing the w_0, the other diameters were calculated with the equation that described the Gaussian beam radius w (x) [42]:

$$w^2(x) = {w_0}^2 \left(1 + \left(\frac{\lambda x}{\pi {w_0}^2}\right)^2\right)$$

x being the distance where the diameter is calculated from the focus of the lens.

A graph, figure 31, was plotted with the results of the theoretical diameter, in order to see if the Gaussian beam distribution affected or not the measured area.

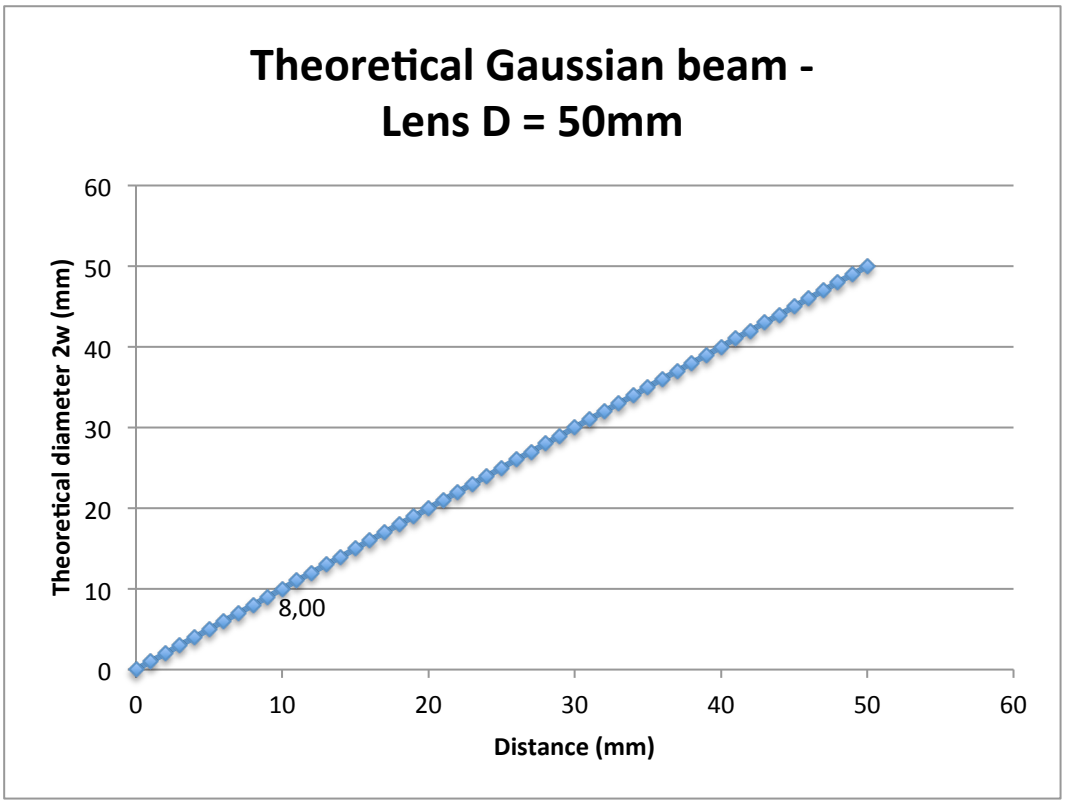

Figure 31. The graph plots the theoretical diameter of the Gaussian beam in different distances.

The theoretical results showed that the Gaussian distribution of the beam shouldn't affect the measured area, as the diameter at 8 mm of distance, where the cornea has to be placed, should be over 8 mm.

- *The Laser*

Once the Gaussian beam distribution was discarded, the laser was tested as a cause of the reduced beam diameter. The laser was changed for another one with different features. The diameter of the beam was measured again using the camera's sensor, and the results were also plotted in the following graph, figure 32.

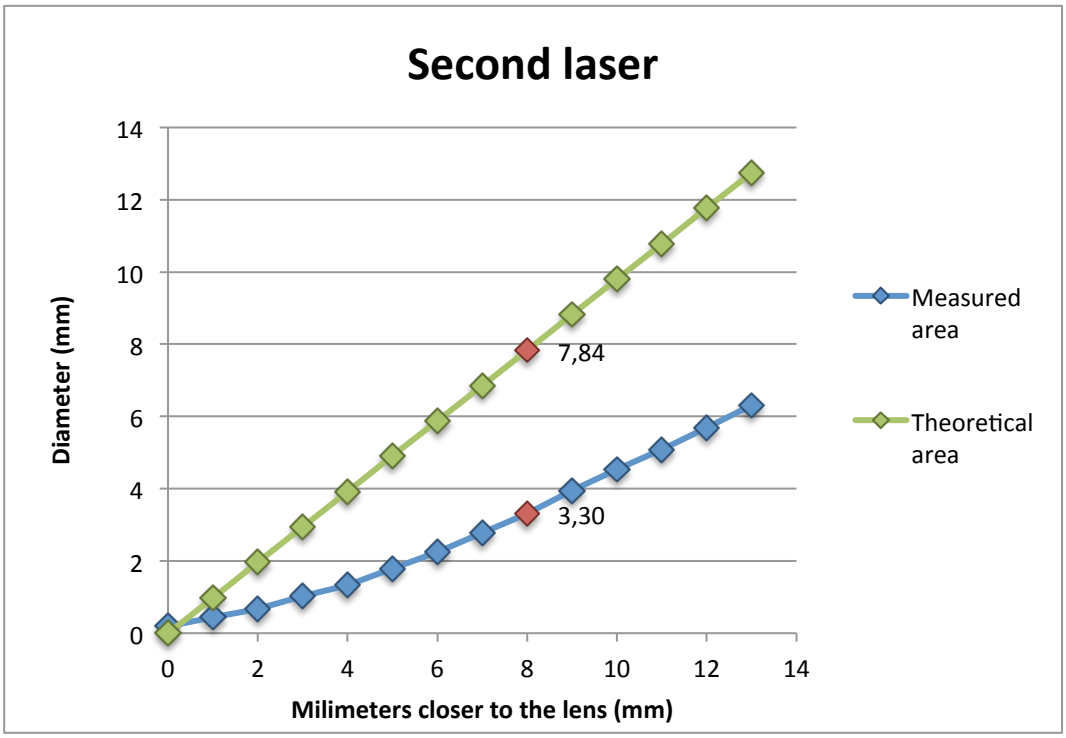

Figure 32. The graphs plots the diameter obtained changing the laser if the distance between the lens and the camera decreases.

Although the diameter was slightly bigger than with the other laser, 3.30 mm at 8 mm of the focus, the behaviour of the beam was almost the same as with the previous laser. Consequently, the laser was not the element causing the problems with the measured area.

- *The incidence lens*

Finally, the last option considered was to change the incidence lens and prove whether it affected the measured area. For this reason, two different lenses were settle at the incidence lens position, and the diameter at different distances was measured.

The first graph, figure 33, shows both the theoretical area and the measured area using a lens (nº 1) with a focal length of 150 mm, and a diameter of 50 mm. And the second graph, figure 34, shows the same but using a lens (nº 2) with a focal length of 60 mm and a diameter of 60 mm.

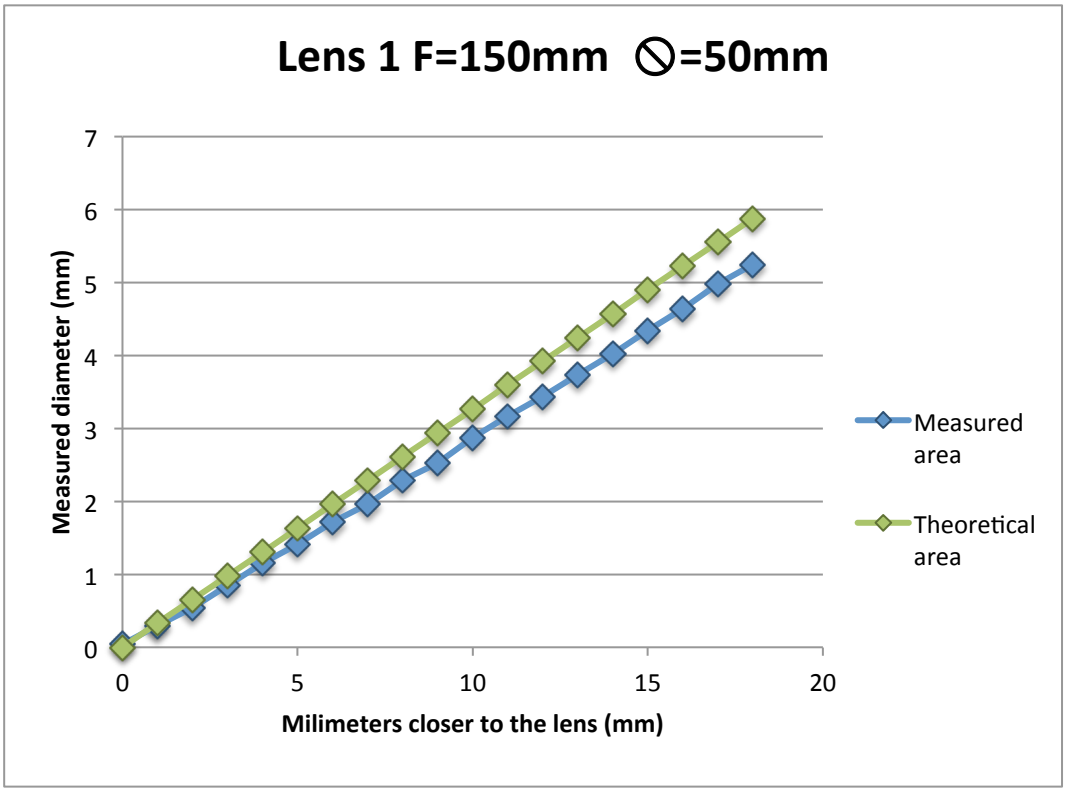

Figure 33. The graphs plots the diameter obtained using a lens with F=150mm, if the distance between the lens and the camera decreases.

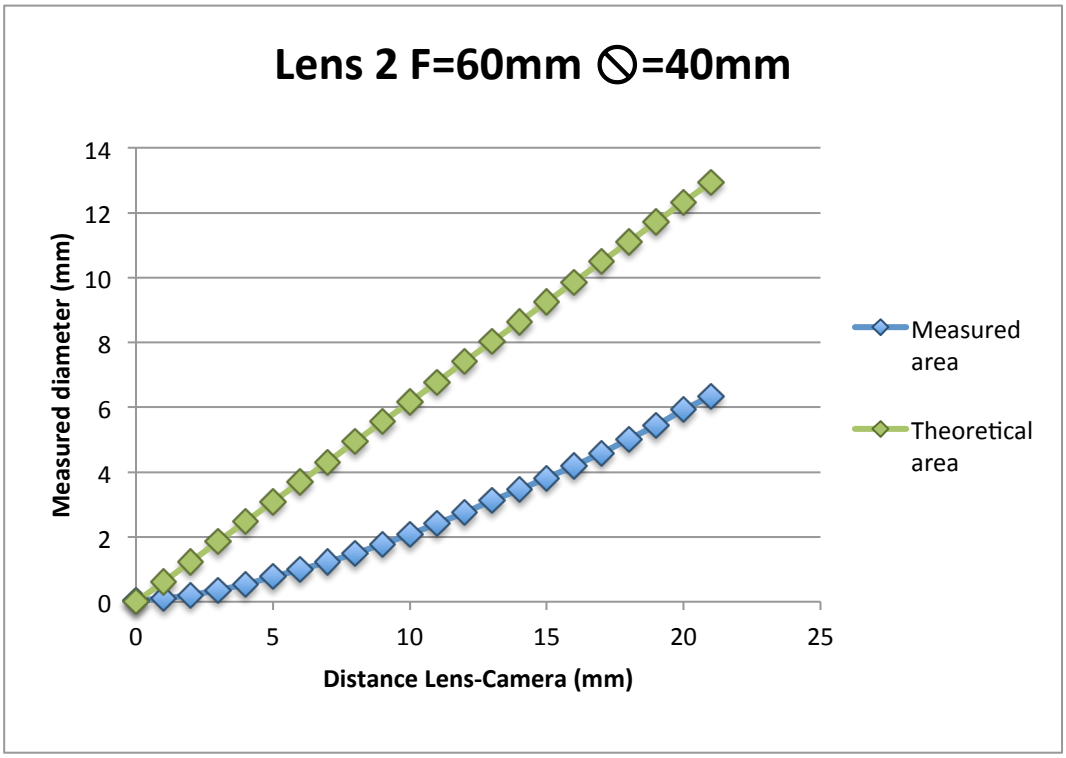

Figure 34. The graphs plots the diameter obtained using a lens with F=60mm, if the distance between the lens and the camera decreases.

The behaviour of the beam using the lens nº 2 is the same as with the original lens, the diameter doesn't increase linearly and is smaller than it should be. However, using the lens nº 1, the beam acts as it should accordingly to the theory. According to these results it could be thought that the problem is due to some of the characteristics of the incidence lens, which the lens nº 2 might also have, as the short focal length.

3.3 Sensitivity to patient displacement

During the setup construction and the following taken measurements, it was observed that the setup could be sensitive to some displacements of the artificial eye in the z-axis.

In clinical practice, this is a relevant aspect to take into account when choosing a technique due to the patient movement. Therefore, it was considered to take some measurements of how the image changed if the eye moved in this axis.

To check how the image changed when the patient moved, the artificial eye was settled in its position, with no displacement relative to the optimum position, z=0. With this configuration, while the artificial eye was moved in steps of 1 mm in the z-axis, pictures were recorded for each of the positions. For every recorded image, the size was calculated (as previously done) by means of the uEye software. The results obtained are shown in figure 35 and table 9:

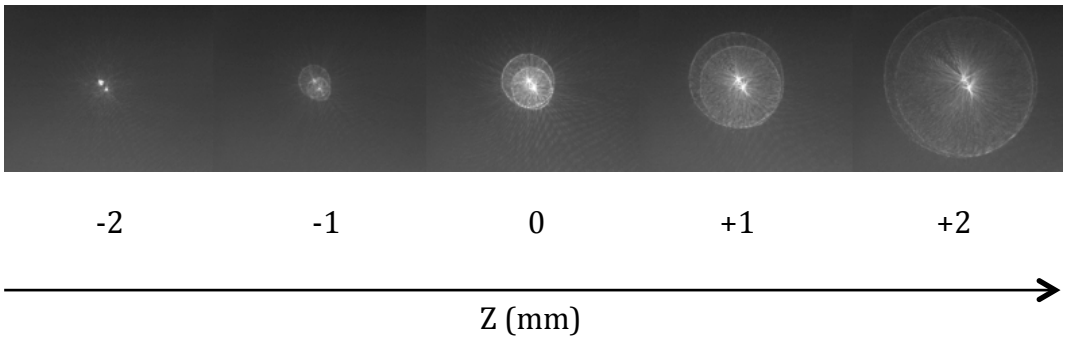

Figure 31. Sequence on images of the artificial eye with steps of 1 mm forward to the lens.

Distance (mm)	Nº of pixels	Diameter (mm)	% of the 0 position
-2	35	0,1855	11,2903
-1	190	1,007	61,2903
0	310	1,643	100
+1	565	2,9945	182,2580
+2	905	4,7965	291,9354

Table 9. Results of the changing diameter when the distance varies.

From the results, it can be interpreted that the image changes dramatically with a displacement of only 1 millimetre. For instance, when the artificial eye was one millimetre closer to the lens, the image increased almost twice the size of the original image. On the contrary, when the artificial eye was one millimetre further, the image decreased half the size of the original image. When the displacement was even bigger than 1 millimetre, the size of the image was significantly different from the original, as it can be seen in the last column of the table 9.

A theoretical calculation of how the image changed if the distance between the eye and the lens was different, was performed counting on Mikel Aldaba's help, to compare the results with the practical ones, and as shown in table 10, they were fairly similar.

Distance (mm)	D_%	Theoretical D_%
-2	11,2903	1925
-1	61,2903	87,1287
0	100	100
1	182,2580	177,6357
2	291,9354	222,7272
3	395,1612	253,3562

Table 10. Effective % of changing size vs. theoretical % of the changing size of the image.

There was only one effective result that didn't correlate with the theoretical one; this was the result at the distance -2mm. As it can be seen, the theoretical image increases dramatically and the effective one doesn't. However, when the measurements were taking place, it was observed that going backwards to -2 mm, the image seemed to increase a lot.

Consequently, the technique indicates a significant sensitivity to patient displacement that could imply an important drawback in clinical practise.

4. CONCLUSIONS AND DISCUSSION

This work aimed to create a new design that permitted an increase of the measured area of the previous setup done for Mikel Aldaba *et al.* at CD6 for DED diagnose.

Theoretically, the proposed setup was capable of increasing the measured diameter to 8mm from the previous configuration, while the effective diameter was 2,19 mm. These results did not correlate with the ones proposed by Licznerski [36] and Dubra [27] where it was ensured that an 8 mm measured area was obtained with this configuration. The reason why the effective diameter was smaller than it should be is still not certain, but it could be due to some of the factors treated in the results and discussed above.

First of all, it was believed that the Gaussian beam distribution could affect to the size of the measured area. Therefore, a new configuration with a pinhole and a diffusor was settled on the setup, which tried to improve the intensity distribution of the beam, and therefore the measured area. This new configuration didn't work properly and it was decided to calculate the theoretical Gaussian beam to see whether it affected. Having the theoretical measurements of the Gaussian beam, it was concluded that the Gaussian intensity distribution should not modify the diameter of the beam.

In the second place, a new laser was used to see if this was the origin of the issue. Although the results of the measured area were slightly bigger, the behaviour of the beam was still the same as with the previous laser; the effective diameter was half of the theoretical one, and with distance it didn't increase linearly. For these reasons, it was confirmed that the laser was not the problem of having a smaller measured area.

Seeing that none of the elements tried before was the problem, it was finally decided to study the effect of different lenses instead on the original incidence lens, and observe the beam's behaviour. The light acted in the same way as with the original lens when the lens number 2 was tried, while with the lens number 1 the beam behaved as theoretically had to. These results lead to believe that the lens could be the focus of the problem, due to some of its characteristics, which the lens nº 2 might have but not lens nº 1. These features could correspond to some aberrations produced due to the size of the lens, or may be to the short focal length accordingly to the diameter. However, is hasn't been tested and this are only suppositions that could be helpful for future works on this field.

In addition to the small diameter, the setup was sensitive to small changes on the position of the patient. That is a considerable drawback when talking about using the technique in clinical practise. The human body is constantly moving and is very difficult to stay still. Therefore, this could lead to a difficult procedure when measuring the NIBUT with this new technique making it inappropriate for the project purpose.

Within this project it has been worked for the improvement on the size of the measured area of a new technique that was started for a laboratory group in CD6, so as to diagnose DED measuring the tear film stability. The new design it was based on configuration a proposed by Licznerski [36] and Dubra [27]. However, the conducted tests demonstrate that the measured area described by Licznerski and Dubra and supported for the theory, is not the area obtained in the constructed setup. Having considered a number of causes that could explain the reduced area, no clear explanation has been found for the differences between the effective results and what the theory and other authors say. Nevertheless, our results suggest that the incidence lens could play a role and future work in this line could lead to a solution of the found problem. Moreover, it has been observed a significant change on the image with only a 1 mm

movement of the patient. For this reason, it is believed that this is another aspect to work with for the improvement of this new technology.

5. BIBLIOGRAPHY

1. Willcox MDP, Argüeso P, Georgiev GA, Holopainen JM, Laurie GW, Millar TJ, et al. TFOS DEWS II Tear Film Report. Ocul Surf [Internet]. 2017;15(3):366–403.

2. Eye ID. The definition and classification of dry eye disease: report of the Definition and Classification Subcommittee of the International Dry Eye WorkShop (2007). Ocul Surf [Internet]. 2007 Apr;5(2):75–92.

3. Gayton JL. Etiology, prevalence, and treatment of dry eye disease. Clin Ophthalmol. 2009;3(1):405–12.

4. Stapleton F, Alves M, Bunya VY, Jalbert I, Lekhanont K, Malet F, et al. TFOS DEWS II Epidemiology Report. Ocul Surf [Internet]. 2017;15(3):334–65.

5. Sullivan DA, Rocha EM, Aragona P, Clayton JA, Ding J, Golebiowski B, et al. TFOS DEWS II Sex, Gender, and Hormones Report. Ocul Surf [Internet]. 2017;15(3):284–333.

6. Wolff E: The mucocutaneous junction of the lid margin and the distribution of the tear fluid. Trans Ophthalmol Soc UK 1946;66:291-308

7. University of Rochester Medical Center. The ocular surface and tear film. 1954;

8. King-Smith PE, Fink BA, Fogt N, Nichols KK, Hill RM, Wilson GS. The thickness of the human precorneal tear film: Evidence from reflection spectra. Investig Ophthalmol Vis Sci. 2000;41(11):3348–59.

9. Tiffany J. The normal tear film. Dev Ophthalmol. 2008;41:1–20.

10. Lemp MA, R. Marquardt. The Dry Eye.

11. Braun RJ. Dynamics of the tear film. Annu Rev Fluid Mech 2012;44. 267, 97.

12. Wolffsohn JS, Arita R, Chalmers R, Djalilian A, Dogru M, Dumbleton K, et al. TFOS DEWS II Diagnostic Methodology report. Ocul Surf [Internet]. 2017;15(3):539–74.

13. Koh S. Mechanisms of Visual Disturbance in Dry Eye. Cornea [Internet]. 2016 Nov;35 Suppl 1(11):S83–8.

14. P. Cho, “Stability of the precorneal tear film: a review,” Clin. Exp. Optom. 74, 19–25 (1991).

15. P. E. King-Smith, B. A. Fink, R. M. Hill, K. W. Koelling, and J. M. Tiffany, “The thickness of the tear film.” Curr. Eye Res. 29, 357–68 (2004)

16. Jesse Vislisel M. Tear breakup time (TBUT) [Internet]. 2015. Available from:https://webeye.ophth.uiowa.edu/eyeforum/atlas/pages/TBUT/index.htm

17. Tomasz J. Licznerski, Henryk T. Kasprzak, Waldemar Kowalik, "Analysis of shearing interferograms of tear film by the use of fast Fourier Transforms," J. Biomed. Opt. 3(1) (1 January 1998)

18. Optometrists CS. Assessment and Diagnosis of Dry Eye [Internet]. Available from: https://www.collinsoptometrists.com.au/dry-eye-clinic/assessment/#OSDIQ

19. Hirsch JD, Reis BL. Reliability and Validity of the Ocular Surface Disease Index. Arch Ophthalmol. 2000;118(May):615–21.

20. Murube del Castillo. Ojo seco. Mesa Redonda 73 Congreso de la SEO. [serie en Internet] 1997 [citado 14 de febrero de 2003]. Disponible en: http://www.oftalmored.com/ojoseco/indice.htm

21. Senchyna M, Wax MB. Quantitative assessment of tear production: A review of methods and utility in dry eye drug discovery. J Ocul Biol Dis Infor. 2008;1(1):1–6.

22. Bron AJ. Diagnosis of Dry Eye. Surv Ophthalmol [Internet]. 2001 Mar;45(March):S221–6.

23. Bron AJ, Evans VE, Smith JA. Grading of corneal and conjunctival staining in the context of other dry eye tests. Cornea. 2003;22(7):640–50.

24. Kojima T, Ishida R, Dogru M, Goto E, Takano Y, Matsumoto Y, et al. A new noninvasive Tear Stability Analysis System for the assessment of dry eyes. Investig Ophthalmol Vis Sci. 2004;45(5):1369–74.

25. Renishaw. Interferometry explained [Internet]. Available from: https://www.renishaw.com/en/interferometry-explained--7854

26. Sweeney DF, Millar TJ, Raju SR. Tear film stability: A review. Exp Eye Res. 2013;117:28–38.

27. Alfredo Dubra, Carl Paterson, and Christopher Dainty, "Study of the tear topography dynamics using a lateral shearing interferometer," Opt. Express 12, 6278-6288 (2004)

28. Shearing Interferometer [Internet]. Available from: https://en.wikipedia.org/wiki/Shearing_interferometer

29. Ibrahim OMA, Dogru M, Takano Y, Satake Y, Wakamatsu TH, Fukagawa K, et al. Application of visante optical coherence tomography tear meniscus height measurement in the diagnosis of dry eye disease. Ophthalmology [Internet]. 2010;117(10):1923–9.

30. Werkmeister RM, Hermand J-P, Aranha dos Santos V, Schmidl D, Gröschl M, Unterhuber A, et al. In vivo tear film thickness measurement and tear film dynamics visualization using spectral domain optical coherence tomography. Opt Express. 2015;23(16):21043.

31. Werkmeister RM, Aschinger G, Messner A, Gröschl M, Schmidl D, Aranha dos Santos V, et al. Super-resolved thickness maps of thin film phantoms and in vivo visualization of tear film lipid layer using OCT. Biomed Opt Express. 2016;7(7):2650.

32. Benito A, Pérez GM, Mirabet S, Vilaseca M, Pujol J, Marín JM, et al. Objective optical assessment of tear-film quality dynamics in normal and mildly symptomatic dry eyes. J Cataract Refract Surg. 2011;37(8):1481–7.

33. Mihashi T, Hirohara Y, Koh S, Ninomiya S, Maeda N, Fujikado T. Tear film break-up time evaluated by real-time Hartmann-Shack wavefront sensing. Jpn J Ophthalmol. 2006;50(2):85–9.

34. Mikel Aldaba, Alejandro Mira-Agudelo, John Fredy Barrera Ramírez, Carlos Enrique García-Guerra, and Jaume Pujol Ramo, "Tear film stability assessment by corneal reflex image degradation," J. Opt. Soc. Am. A 36, B110-B115 (2019)

35. Craig JP, Willcox MDP, Argüeso P, Maissa C, Stahl U, Tomlinson A, et al. The TFOS International Workshop on Contact Lens Discomfort: Report of the Contact Lens Interactions With the Tear Film Subcommittee. Investig Opthalmology Vis Sci [Internet]. 2013 Oct 18;54(11):TFOS123.

36. T. J. Licznerski, H. T. Kasprzak, and W. Kowalik, “Analysis of shearing interferograms of tear film by the use of fast Fourier Transforms,” J. Biomed. Opt. 3(1), 32–37 (1998).

37. Edmund Optics [Internet]. 2019. Available from: https://www.edmundoptics.com

38. IDS Imaging Development Systems Gmbh. 2019; Available from: https://en.ids-imaging.com/home.html

39. Doughty MJ, Zaman ML. Human Corneal Thickness and Its Impact on Intraocular Pressure Measures. Surv Ophthalmol. 2002;44(5):367–408.

40. Nave R. Scale model of Eye [Internet]. Available from: http://hyperphysics.phy-astr.gsu.edu/hbase/vision/eyescal.html

41. NUS Physics. Propagation of Laser Beam [Internet]. Available from: https://www.physics.nus.edu.sg/pc2193/Experiments/lab.pdf

42. Newport. Gaussian Beam Optics [Internet]. 2019. Available from: https://www.newport.com/n/gaussian-beam-optics

43. QUESTTEL. Numerical aperture in fiber optics [Internet]. 2019. Available from: https://questtel.com/wiki/numerical-aperture-in-fiber-optics